

# NATIONAL TRANSPORTATION SAFETY BOARD

Office of Research and Engineering  
Washington, D.C. 20594

December 6, 2017

## Aircraft Performance Radar & Simulation Study

by John O'Callaghan

### A. ACCIDENT

Location: Amarillo, TX

Date: April 28, 2017

Time: 23:48 Central Daylight Time (CDT)<sup>1</sup>

Aircraft: Pilatus Aircraft Ltd. PC-12, registration N933DC

NTSB#: CEN17FA168

### B. GROUP

Not Applicable

### C. HISTORY OF FLIGHT

On April 28, 2017, about 23:48 CDT, a Pilatus PC-12 airplane, N933DC, impacted terrain near Rick Husband Amarillo International Airport (KAMA), Amarillo, Texas. The airline transport pilot and two flight crew were fatally injured. The airplane was destroyed. The airplane was registered to and operated by Rico Aviation LLC, under the provisions of 14 Code of Federal Regulations Part 135 as an air ambulance flight. Instrument meteorological conditions (IMC) prevailed at the time of the accident and the flight was operated on an instrument flight rules (IFR) flight plan. The flight was originating at the time of the accident and was en route to Clovis Municipal Airport (KCVN), Clovis, New Mexico.

This *Aircraft Performance Radar & Simulation Study* presents the results of using Amarillo Airport Surveillance Radar (AMA ASR) data, evidence at the crash site, wind data derived from another aircraft, Air Traffic Control (ATC) communications, and simulation results to estimate the position and orientation of the airplane during the accident flight. The simulation results provide a trajectory that is consistent with both the recorded radar data, and the performance capabilities of the airplane. The simulation also yields a set of control and throttle inputs that are consistent with the simulated trajectory (though it should be noted that other inputs, which produce similar but slightly different trajectories, could also be generally consistent with the recorded radar data).

A simulation of the flight that approximately matches the radar data describes the following sequence of events concerning the accident flight. In what follows, "the airplane" or "N933DC"

---

<sup>1</sup> Local time at Amarillo on the day of the accident was Central Daylight Time (CDT). CDT = UTC - 5 hours. Times in this *Study* are in CDT unless otherwise noted.

refers to the *simulated* airplane, and the behavior described is a reasonable estimate of N933DC's *actual* behavior based on the simulation. However, the simulation results, while very precise, are only *estimates* based on an *approximate* match of the radar data, that are themselves *approximate* measurements of N933DC's position as a function of time. These caveats, and the uncertainties they imply, should be considered in the description that follows, and in the simulation results plotted in the various Figures referred to in this *Study*. The simulation itself is described in greater detail in Section D-IV.

The simulation indicates that after lifting off from KAMA runway 4, N933DC accelerated to about 193 KCAS while climbing between 600 and 1200 ft/min to an altitude of about 4400 ft above Mean Sea Level (MSL), or about 800 ft above ground level (AGL). The airplane leveled at 4300 to 4400 ft MSL until about 23:46:30, when it resumed climbing, reaching 6000 ft MSL (2400 ft AGL) at about 23:46:52. During this climb, the airplane decelerated from 193 KCAS to about 122 KCAS. At about 23:47:02, the airplane started an increasingly rapid descent from 6000 ft MSL to the ground (elevation 3600 ft MSL). The estimated rate of descent and airspeed at impact (based on simulation) are about 17000 ft/min and 220 KCAS, respectively. The estimated time of impact is about 23:47:19.

At about 23:45:42, while climbing through 4100 ft MSL (500 ft AGL), the airplane started a slow roll to the right, reaching a roll angle of about  $42^\circ$  at about 23:46:10. At 23:46:24 the roll angle had decreased to  $36^\circ$ , and the pitch angle started to increase steadily (consistent with the climb to 6000 ft MSL). At 23:46:32, when the roll angle was  $30^\circ$ , the airplane started rolling more quickly to the left, rolling through wings level at about 23:46:40 (then on a ground track of  $267^\circ$  true). The airplane achieved a peak pitch angle of about  $23^\circ$  at about 23:46:42, after which the pitch angle decreased steadily to an estimated  $-42^\circ$  at impact. As the pitch angle decreased, the roll angle increased steadily to the left, reaching an estimated  $-76^\circ$  at impact.

The simulation requires full throttle from 23:45:24 through 6000 ft MSL, except for two brief power reductions between 23:45:48 and 23:45:56 and between 23:46:28 and 23:46:30, when there is a pause in the increase in airspeed and the airplane levels briefly at 4400 MSL.

The simulation control inputs are well within the airplane's control travel limits, and the computed column and wheel control forces required are generally (until the last 7 seconds of the flight) within the one-hand short-term force limit prescribed in 14 Code of Federal Regulations (CFR) paragraph 23.143 (§23.143). The simulation maximum normal load factor, reached at impact, was about 2.6 G's. In addition, throughout the flight the simulation lift coefficient ( $C_L$ ) remained below the flaps-up maximum  $C_L$  ( $C_{Lmax}$ ) implied by the flaps-up stall speed published in the Airplane Flight Manual (AFM), indicating that the airplane could fly the trajectory indicated by the radar data without stalling.

An estimate of the "apparent" pitch and roll angles, representing the attitude a pilot would "feel" the airplane to be in based on his vestibular / kinesthetic perception of the components of the load factor vector in his own body coordinate system, was made based on the simulation load factors. The "apparent" pitch angle ranged between  $0^\circ$  and  $15^\circ$ , and the "apparent" roll angle ranged between  $0^\circ$  and  $-4^\circ$ .

The details of the performance estimates based on radar data, the simulation match of the radar data, and the calculation of the "apparent" pitch and roll angles are provided in the sections below.

## D. DETAILS OF THE INVESTIGATION

### I. Airplane position based on radar data

#### *Description of ARSR and ASR Radar Data*

In general, two types of radar are used to provide position and track information for aircraft cruising at high altitudes between airport terminal airspaces, and for those operating at low altitude and speeds within terminal airspaces.

Air Route Surveillance Radars (ARSRs) are long range (250 nmi) radars used to track aircraft cruising between terminal airspaces. ARSR antennas rotate at 5 to 6 RPM, resulting in a radar return every 10 to 12 seconds. Airport Surveillance Radars (ASRs) are short range (60 nmi) radars used to provide air traffic control services in terminal areas. ASR antennas rotate at 13 to 14 RPM, resulting in a radar return every 4.3 to 4.6 seconds. Radar returns from N933DC recorded by the ASR at KAMA (see Figure 1) are the basis for the trajectory and performance calculations and simulation presented in this *Study*.

#### *Primary and Secondary Radar Returns*

A radar detects the position of an object by broadcasting an electronic signal that is reflected by the object and returned to the radar antenna. These reflected signals are called *primary returns*. Knowing the speed of the radar signal and the time interval between when the signal was broadcast and when it was returned, the distance, or range, from the radar antenna to the reflecting object can be determined. Knowing the direction the radar antenna was pointing when the signal was broadcast, the direction (or bearing, or azimuth) from the radar to the object can be determined. Range and azimuth from the radar to the object define the object's position.

The strength or quality of the return signal from the object depends on many factors, including the range to the object, the object's size and shape, and atmospheric conditions. In addition, any object in the path of the radar beam can potentially return a signal, and a reflected signal contains no information about the identity of the object that reflected it. Many times, these difficulties make distinguishing individual aircraft from each other and other objects (e.g., flocks of birds) based on primary returns alone unreliable and uncertain.

To improve the consistency and reliability of radar returns, aircraft are equipped with transponders that sense beacon interrogator signals broadcast from radar sites, and in turn broadcast a response signal. Thus, even if the radar site is unable to sense a weak reflected signal (primary return), it will sense the response signal broadcast by the transponder and be able to determine the aircraft position. The response signal can also contain additional information, such as the identifying "beacon code" for the aircraft, and the aircraft's pressure altitude (also called "Mode C" altitude). Transponder signals received by the radar site are called *secondary returns*. N933DC was assigned a beacon code of 4261, though it took off broadcasting code 4254, and switched to code 4261 after a request from ATC at 23:46:11.

#### *Recorded Radar Data*

Recorded data from the AMA ASR was obtained from the Federal Aviation Administration (FAA), and includes the following parameters:

- UTC time of the radar return, in hours, minutes, and seconds.
- Transponder beacon code associated with the return (secondary returns only)
- Transponder reported altitude in hundreds of feet associated with the return (secondary returns only). The transponder reports pressure altitude. The altitude recorded in the file depends on the site recording the data; some sites record both pressure altitude, and pressure altitude adjusted for altimeter setting (MSL altitude). Others record just the MSL altitude. The file for this case contains both. The altimeter setting for the time of the accident (29.78 "Hg) results in a pressure altitude about 129 ft higher than the MSL altitude; however, the MSL altitudes recorded in the radar file are 200 ft lower than the pressure altitudes, but match the KAMA elevation during the takeoff roll.<sup>2</sup> Consequently, the corrected MSL altitudes as recorded in the file are used at the target altitudes for the simulation described in this *Study*. The resolution of the altitude data in the radar file is  $\pm 50$  ft.
- Slant Range from the radar antenna to the return, in nmi. The accuracy of this data is  $\pm 1/16$  nmi or about  $\pm 380$  ft.
- Azimuth relative to magnetic north from the radar antenna to the return. The AMA ASR uses a magnetic variation of  $8^\circ$  E to determine magnetic azimuth. Azimuth is reported in Azimuth Change Pulses (ACPs). ACP values range from 0 to 4096, where  $0 = 0^\circ$  magnetic and  $4096 = 360^\circ$  magnetic. Thus, the azimuth to the target in degrees would be:

$$(\text{Azimuth in degrees}) = (360/4096) \times (\text{Azimuth in ACPs}) = (0.08789) \times (\text{Azimuth in ACPs})$$

The accuracy of azimuth data is  $\pm 2$  ACP or  $\pm 0.176^\circ$ .

- The latitude and longitude of the return computed by the radar system data processing algorithms. The latitude and longitude reported in the file is slightly different than what would be computed from the range and azimuth data recorded in the file (see below).

To determine the latitude and longitude of radar returns from the range and azimuth data recorded by the radar, the geographic location of the radar antenna must be known. The coordinates of the AMA ASR antenna are:

35° 12' 54.829" N latitude; 101° 42' 35.48" W longitude; elevation 3722 feet

### *Presentation of the Radar Data*

To calculate performance parameters from the radar data (such as ground speed and track angle), it is convenient to express the position of the airplane in rectangular Cartesian coordinates. The Cartesian coordinate system used in this *Study* is centered at the KAMA runway 4 threshold and its axes extend east, north, and up from the center of the Earth. The data from the AMA radar is converted into this coordinate system for plotting and performance calculations. Latitude and longitude coordinates are transformed into this coordinate system using the WGS84 ellipsoid model of the Earth.

Figures 1 and 2 show the AMA ASR data plotted in terms of nautical miles north and east of the runway 4 threshold. Figure 1 shows the data with a Cartesian grid background, and Figure 2 shows the data with a *Google Earth* satellite image background. The ATC communications with N933DC, taken from Reference 3 and listed in Table 1, are also plotted in Figures 1 and 2 at the locations along N933DC's flight track at which they occurred.

---

<sup>2</sup> Rounding the MSL altitude to the nearest 100 ft, the recorded MSL altitudes would be expected to be 100 ft lower than the recorded pressure altitudes, instead of 200 ft lower (-129 ft rounds to -100 ft, not -200 ft). The reason for this 100 ft discrepancy was not determined.

A three-dimensional Google Earth representation of the simulation solution that approximately matches the radar and crash site data is shown in Figure 3. The blue labels in the Figure indicate the simulation time, MSL altitude, calibrated airspeed, and rate of climb corresponding to the position of each airplane in the Figure. The orientation of each airplane (drawn larger than their correct proportions for greater visibility) indicate the heading, pitch, and roll angles computed by the simulation at those points. The green labels in Figure 3 indicate the time and MSL altitude of the AMA ASR returns.

The north and east positions of the AMA ASR beacon code 4254 and 4261 returns are shown as a function of time in Figure 4, along with the simulation positions. The altitude of the airplane, as determined from the Mode C transponder returns, is shown as a function of time in Figure 5, along with the simulation altitude. The shaded areas of Figure 5 indicate the sky condition as reported in the KAMA 04:53 UTC (23:53 CDT) METAR report, and listed in Table 2.

The latitude and longitude recorded in the radar data file differ slightly from the latitude and longitude computed using the range and azimuth data recorded in the file; the former are consistent with range values about 0.023 nmi (140 ft) greater than the range values recorded in the file. The reason for this range difference is unknown, but may be the result of a small error in the position of the radar antenna in the radar processing algorithms. In any case, the computed latitude and longitude place N933DC closer to the runway centerline during the takeoff roll and initial climb than do the recorded latitude and longitude, which place the airplane slightly northwest of the runway. Hence, the computed latitude and longitude are likely more representative of the airplane's true position than the recorded latitude and longitude, and so the performance work described in this *Study* (including the target trajectory for the simulation) is based on the computed latitude and longitude data.

The AMA ASR data, along with the (computed) latitude, longitude, north and east coordinates for each radar return are tabulated in Tables 3a (for beacon code 4254) and 3b (for beacon code 4261).

## II. Crash site and winds aloft information

### *Crash site information*

The latitude and longitude coordinates of the crash site were recorded on-scene by NTSB investigators. According to the preliminary NTSB report of the accident (Reference 1),

The airplane impacted a pasture ([see] Figure [6]) adjacent to several stationary train cars about 1 nautical mile south of AMA and a post impact fire ensued. The wreckage debris path was generally oriented southwest. All major structural components of the airplane were located within the wreckage.

Based on a survey of the debris field, the impact location was determined to be:

Latitude 35°11'46.45" N (0.532 nm south of the KAMA runway 4 threshold)  
 Longitude 101°42'16.46" W (1.383 nm east of the KAMA runway 4 threshold)  
 Elevation 3607 ft MSL (per *Google Earth*)

These are the "crash site" coordinates plotted in Figures 1 and 2. Figures 6 and 7 are photographs of the crash site, viewed from different directions.

### *Winds aloft information*

Winds aloft for the simulation were modelled based on wind and other information recorded on the Flight Data Recorder (FDR) of a Boeing 737 (B737) that departed KAMA about one hour after the accident time. The B737 FDR recorded wind data from two different sources: the Flight Management Computer (FMC), and the Inertial Reference System (IR-3). In addition, winds were computed by the NTSB using the groundspeed, ground track, heading, and airspeed parameters recorded on the FDR.

A curve fit through the NTSB calculated winds and adjusted to match the recorded B737 FMC and IR-3 winds was used in the simulation of the accident. Figure 8 shows the recorded winds and the winds used in the simulation plotted as a function of altitude.

The static air temperature recorded on the B737 FDR was invalid, so this parameter was computed based on the recorded total air temperature, airspeed, and pressure altitude parameters. The calculated static air temperature is plotted as a function of altitude in Figure 8, and was used in the simulation of the accident.

### **III. Weight and balance information**

Rico Aviation provided the NTSB with weight and balance information for the accident flight, including the empty weight and center of gravity (CG) position of the airplane, the weight of the pilot, the weights and likely seating positions of the two flight crew, and the amount of fuel aboard the airplane. This information, and the resulting takeoff weight and CG values, are shown in Table 4. The computed takeoff weight of 9328 lb. is below the maximum allowable takeoff weight of 9921 lb specified in the PC-12 AFM (Reference 2<sup>3</sup>), and the computed CG position of 236.3 inches is between the allowable CG range of about 229.5 to 241.5 inches (at 9328 lb). The takeoff weight and CG shown in Table 4 were used in the simulation of the accident flight.

Additional mass properties used in the simulation are shown in Table 5, and include the vertical and lateral CG positions, and the moments of inertia. The lateral CG position was assumed to be at the centerline, and the vertical CG position and moments of inertia were estimated based on exemplar cargo and fuel load scenarios provided by Pilatus.

A three-view drawing of the Pilatus PC-12, taken from Reference 2, is shown in Figure 9.

### **IV. Airplane performance calculations based on flight simulation**

As mentioned above, a computer simulation of the accident flight was performed in order to generate a trajectory that is consistent with both the recorded radar data and crash site location, and the performance capabilities of the airplane. The simulation also yields a set of control and throttle inputs that are consistent with the simulated trajectory (though it should be noted that other inputs, which produce similar but slightly different trajectories, could also be generally consistent with the recorded radar data).

---

<sup>3</sup> The manufacturer's serial number (MSN) of N933DC was 105, corresponding to a maximum gross weight of 9039 lb. However, in June 2000 the airplane was modified to conform to the PC-12/45, with an increased gross weight of 9921 lb. The AFM corresponding to this higher gross weight is referenced here.

The following information sources define the “target” trajectory and airplane model used in the simulation, and provide criteria by which to measure the quality of the simulation match:

**Radar data:** For the simulation to “match” the radar data, the position of the airplane in the simulation solution should lie within the uncertainty boxes of the radar returns at the times corresponding to those returns, and the altitude should fall between the  $\pm 50$  ft. uncertainty band of the corrected Mode C data at those times.

**Crash site data:** The simulation and actual crash sites should coincide.

**Performance data:** The simulation should be representative of the Pilatus PC-12 aerodynamics and engine thrust capabilities. Airplane aerodynamics and engine simulation models provided by Pilatus were used for this *Study*. These models were developed by Pilatus for SimCom (a flight simulator manufacturer), and were largely complete, except for the flight control system. For this system, Pilatus provided system description reports (including control gearing ratios and aerodynamic surface hinge moments) from which a flight control system model could be constructed. As described further below, the resulting model yielded reasonable control forces in the pitch and yaw axes, but did not yield reasonable control forces in the roll axis. For the roll control forces, a simpler, linearized model provided to the NTSB for a previous PC-12 accident investigation was used, and this model did yield reasonable roll control forces.

**Wind data:** The winds and temperatures aloft as a function of altitude, based on the B737 FDR data described above, were used in the simulation.

The simulation uses a “math pilot” to generate control system and throttle inputs to produce pitch and roll angles and engine thrust that result in an approximate match of the “target” trajectory defined by the radar data and the impact point. Since the aerodynamic characteristics of the simulation are representative of the airplane, the engine power, angle of attack, Euler angles (pitch, roll, and heading), and control inputs and forces computed by the simulation to match the target track are relevant and of interest.

The flaps and gear up configuration is used throughout the simulation, which starts at 23:45:13 with the airplane climbing at about 600 ft/min through 3640 ft. MSL (about 40 ft. AGL) and accelerating through 100 kt. This configuration is consistent with the normal takeoff procedure outlined in the AFM, which states that the gear should be raised after liftoff and positive rate of climb is established, and the flaps should be raised to 0° above 100 kt. The flaps and gear up configuration at the start of the simulation may be a little early (i.e., occur earlier than in the actual flight), which could account for the less than full thrust required at the start of the simulation (see Figure 15). The simulation thrust increases to max power at 23:45:20, so it is likely that the clean configuration was achieved by that time.

The simulation results are presented in Figures 1-5 and 10-18. The results satisfy the match criteria outlined above well, though not perfectly; as shown in Figures 1 and 2, the position of the airplane is within or close to the edge the uncertainty boxes of the radar data at the radar return times, and the impact is close to (about 130 ft from) the crash site. In general, the airplane positions are within about 200 ft of the corresponding radar returns. The attitude of the airplane at impact is: heading 301° true, pitch 42° down, roll 76° left. In this attitude, the projection of the leading edge of the wing along the ground is a line oriented southeast to northwest from 141° to 321°, which matches the general orientation of the ground scar of the left wing leading edge

in the wreckage. The left-wing-low impact attitude is also consistent with the deeper impact crater created by the left wing than the right wing, which is evident in Figures 6 and 7.

Figure 10 shows the speeds computed by the simulation. Note that the simulation ground speed matches the ground speed computed from the AMA ASR returns quite well until about 23:46:40, when the airplane climbs through 5300 ft, though even after this time the simulation and radar speed trends are similar. The magnitude of the decrease in the radar-based ground speed starting around 23:47:00 may be excessive (dropping to 90 kt at the end of the data), since the groundspeed at a given radar point is computed as the average speed along a straight-line segment between the preceding and following radar points. The actual path flown by the airplane is a curved path through all three points, and so is longer than the path used for the radar-based calculation. The magnitude of this error in the radar-based groundspeed calculation increases as the radius of turn of the airplane decreases. The simulation path, being physics-based, is curved, and the groundspeed is correspondingly higher.

As noted above, the simulation starts with the airplane accelerating through an airspeed of 100 KCAS. During the climb to 4400 ft MSL (see Figure 5), the airplane accelerated to about 193 KCAS while climbing between 600 and 1200 ft/min (Figure 10). The airplane leveled at 4300 to 4400 ft MSL until about 23:46:30, when it resumed climbing, reaching 6000 ft MSL at about 23:46:52. During this climb, the airplane decelerated from 193 KCAS to about 122 KCAS. At about 23:47:02, the airplane started an increasingly rapid descent from 6000 ft MSL to the ground. The simulation rate of descent and airspeed at impact are about 17000 ft/min and 220 KCAS, respectively. The estimated time of impact is about 23:47:19.

Figure 11 presents the simulation pitch angle, flight path angle, angle of attack, and roll angle. Figure 12 presents the simulation heading, track, drift, and sideslip angles. At about 23:45:42, while climbing through 4100 ft MSL (500 ft AGL), the airplane started a slow roll to the right, reaching a roll angle of about 42° at about 23:46:10. At 23:46:24 the roll angle had decreased to 36°, and the pitch angle started to increase steadily (consistent with the climb to 6000 ft MSL). At 23:46:32, when the roll angle was 30°, the airplane started rolling more quickly to the left, rolling through wings level at about 23:46:40 (then on a ground track of 267° true). The airplane achieved a peak pitch angle of about 23° at about 23:46:42, after which the pitch angle decreased steadily to an estimated -42° at impact. As the pitch angle decreased, the roll angle increased steadily to the left, reaching an estimated -76° at impact.

The simulation “math pilot” described above also manipulates the rudder pedals so as to target zero lateral acceleration ( $n_y$ ) on the airplane (emulating the activity of the airplane’s yaw damper, though the simulation does not include a model of the yaw damper specifically). There is a large left yawing moment on the airplane due to propeller effects at high power settings, and to balance this yawing moment while achieving (close to) zero  $n_y$ , the simulation requires about 2° to 3° of negative (left) sideslip angle.

Figure 11 also presents the “apparent pitch angle” and “apparent roll angle” that would result from the load factors computed by the simulation, which are presented in Figure 14. These are the pitch and roll angles that an airplane in unaccelerated flight (or equivalently, a pilot seated in a gimbaled chair on the ground) would require to produce load factors in each of the airplane body axes proportional to those plotted in Figure 14. In other words, these are the pitch and roll angles that make the load factor vector in the static case parallel (in airplane body axes) to the load factor vector in the actual accelerated flight case, and represent the attitude a pilot would “feel” the airplane to be in, based on his vestibular / kinesthetic perception of the components

of the load factor vector in his own body coordinate system. Throughout the flight, the “apparent” pitch angle ranged between 0° and 15°, and the “apparent” roll angle ranged between 0° and -4°. The calculation of these angles is described in Section D-V.

The simulation angular rates are presented in Figure 13. Both the rates of change of the Euler angles (pitch, roll, and heading) are shown, along with the body-axis angular rates (i.e., the components of the angular velocity vector along the airplane’s longitudinal (x), lateral (y), and vertical (z) axes). The body-axis angular rates are related to the rates of change of the Euler angles as follows:

$$\begin{Bmatrix} P \\ Q \\ R \end{Bmatrix} = \begin{bmatrix} -\sin \theta & 0 & 1 \\ \sin \phi \cos \theta & \cos \phi & 0 \\ \cos \phi \cos \theta & -\sin \phi & 0 \end{bmatrix} \begin{Bmatrix} \dot{\psi} \\ \dot{\theta} \\ \dot{\phi} \end{Bmatrix} \quad [1]$$

where  $P$ ,  $Q$ , and  $R$  are the body-axis roll, pitch, and yaw rates, respectively, and  $\psi$ ,  $\theta$ , and  $\phi$  are the heading, pitch, and roll angles, respectively. Note that when  $\phi = 0$ ,  $Q = \dot{\theta}$ , and when  $\theta = 0$ ,  $P = \dot{\phi}$ , but in general the body-axis pitch and roll rates are not simply equivalent to the rates of change of the pitch and roll angles. This is apparent in Figure 13, which shows that during the final spiral dive,  $Q$  increases to 15°/s while  $\dot{\theta}$  decreases to -2°/s to -4°/s.

The simulation maximum normal load factor, reached at impact, was about 2.6 G’s (see Figure 14). In addition, throughout the flight the simulation lift coefficient ( $C_L$ ) remained below the flaps-up maximum  $C_L$  ( $C_{Lmax}$ ) implied by the flaps-up stall speed published in the AFM, indicating that the airplane could fly the trajectory indicated by the radar data without stalling (Figure 14). The AFM flaps-up stall speed at a weight of 9921 lb is 93 KCAS. Using the wing reference area of 277.8 ft<sup>2</sup>, the corresponding  $C_{Lmax}$  is 1.22. The maximum  $C_L$  achieved in the simulation was 0.96, reached during the relatively low speed initial climb at the start of the simulation.

Figure 15 shows the engine power parameters computed by the simulation. As noted above, the less-than-full power required at the start of the simulation may be the result of starting the simulation in the clean configuration (flaps and gear up) before the actual airplane achieved this configuration. Otherwise, the simulation requires full throttle from 23:45:24 through 6000 ft MSL, except for two brief power reductions (between 23:45:48 and 23:45:56 and between 23:46:28 and 23:46:30), when there is a pause in the increase in airspeed and the airplane levels briefly at 4400 MSL.

Figures 16, 17, and 18 present the simulation flight control inputs, aerodynamic control surface positions, and flight control forces, respectively. The travel limits of the flight controls and aerodynamic surfaces are also shown in the plots, to provide a sense of the scale of the movements. To provide a scale for the control forces, the short-term force application limits specified in the certification standards for Part 23 airplanes<sup>4</sup> (§23.143) are also shown in Figure 18. §23.143 specifies both 1- and 2-handed force limits for the pitch and roll axes.

The horizontal stabilizer position in the simulation is set at a constant -0.8°, corresponding to the neutral “green sector” marking on the cockpit trim indicator (per Reference 4). Reference 5 indicates that the condition of the horizontal stabilizer actuator in the wreckage “corresponds to a slightly nose-down trim between the neutral setting and the [green diamond] takeoff setting (see ... Figure [19]).

<sup>4</sup> The PC-12 is certified to 14 CFR Part 23 Normal Category standards, through Amendment 23-42.

As mentioned above, the SimCom simulation model yielded reasonable control forces in the pitch and yaw axes, but did not yield reasonable control forces in the roll axis.<sup>5</sup> For the roll control forces, a simpler, linearized model provided to the NTSB for a previous PC-12 accident investigation was used, and this model did yield reasonable roll control forces; this is the “SimuLink” model shown in Figure 18. The SimCom and SimuLink models produced very similar column forces, and somewhat similar pedal forces. The rudder hinge moment coefficients in the SimCom model are multiplied by the thrust coefficient (and so decrease with engine power), but the SimuLink coefficients do not, which accounts for much of the pedal force differences between the models.

The pedal inputs in Figure 16 and the pedal forces in Figure 18 are those that would be required in the absence of any yaw damper activity. The AFM specifies that the yaw damper should be disengaged for takeoff, but that it can be set “as required” after the airplane accelerates past 100 KIAS and the flaps are retracted. Once the yaw damper is engaged, it will provide the rudder inputs required to keep  $n_y$  near zero, and no pedal inputs (or pedal force) will be required from the pilot for this task.

Figures 16-18 indicate that the simulation control inputs are well within the airplane’s control travel limits, and that the column and wheel control forces are generally (until the last 7 seconds of the flight) within the one-hand short-term force limits prescribed in §23.143.

## V. Calculation of the “apparent” pitch and roll angles

As described above, the “apparent” pitch and roll angles presented in Figure 11 represent the attitude a pilot would “feel” the airplane to be in, based on his vestibular / kinesthetic perception of the components of the load factor vector in his own body coordinate system. It is assumed in this case that the pilot perceives attitude by equating the load factor vector with the gravity vector, and resolving his attitude relative to that vector. Because the vestibular / kinesthetic system cannot distinguish load factors resulting from airplane accelerations from load factors resulting from the components of the gravity vector along the body axes, in accelerated flight it is possible for a pilot to misperceive his attitude if he relies on his vestibular / kinesthetic sense alone. This phenomenon is known as the “somatogravic illusion,” and can lead to spatial disorientation.

Figure 20 shows the orientation of the resultant load factor vector  $\vec{n}$  for two cases: in Figure 20a, the airplane is in accelerated flight, and  $\vec{n}$  has a component along the  $x_b$  axis ( $n_x$ ). In Figure 20b, the airplane is unaccelerated, and  $\vec{n}$  is aligned with the gravity vector  $\vec{g}$ , along the earth’s vertical axis ( $z_e$ ). In both cases, the angle of the vector  $\vec{n}$  relative to the airplane’s vertical axis ( $z_b$ ) is the same:  $\theta_{APP}$ . In Figure 20b,  $\theta_{APP}$  is also the actual pitch angle of the airplane axis system, but in Figure 20a, the actual pitch angle  $\theta$  is less than  $\theta_{APP}$ . However, in both cases the pilot’s vestibular / kinesthetic system perceives the pitch angle as  $\theta_{APP}$ . Hence, the perceived  $\theta_{APP}$  matches the actual pitch angle  $\theta$  only when  $\vec{n}$  is aligned with  $\vec{g}$  – i.e., when  $n_x$  and  $n_y$  are zero.

---

<sup>5</sup> The SimCom documentation presented two methods for computing wheel forces: one based on aileron hinge moments and aileron-to-wheel gearing, and another based on an “adimensional yoke force.” As shown in Figure 18, the wheel forces from the first method are unreasonably low (maximum force 5 lb), while those from the second are unreasonably high (they are divided by 100 to fit onto the scale of Figure 18).

To compute  $\theta_{APP}$  and  $\phi_{APP}$ , we seek the pitch and roll angles in an unaccelerated axis system that will produce a vector  $\vec{n}$  parallel (in airplane body axes) to the vector  $\vec{n}$  in the accelerated system. In the unaccelerated system,  $\vec{n}$  has Earth-axis components  $\{0, 0, -g\}$ <sup>6</sup>, or equivalently

$$\vec{n} = \begin{pmatrix} 0 \\ 0 \\ -|\vec{n}| \end{pmatrix}_{EARTH} \quad [2]$$

where

$$|\vec{n}| = \sqrt{(n_x)^2 + (n_y)^2 + (n_z)^2} = g \quad [3]$$

Transforming these components into airplane body axis gives

$$\vec{n} = -|\vec{n}| \begin{pmatrix} -\sin \theta \\ \sin \phi \cos \theta \\ \cos \phi \sin \theta \end{pmatrix}_{BODY} \quad [4]$$

Considering now the accelerated case, the magnitude of the load factor vector  $\vec{n}$  will not, in general, equal the acceleration due to gravity ( $g$ ). However, we seek  $\theta_{APP}$  and  $\phi_{APP}$  such that when the airplane body axis is oriented with these angles in an unaccelerated system (while preserving the magnitude of the load factor vector  $\vec{n}$ ), the resulting body-axis components of  $\vec{n}$  will match the load factors  $n_x$ ,  $n_y$ , and  $n_z$  from the accelerated case. From Equation [4],

$$|\vec{n}| \begin{pmatrix} \sin \theta_{APP} \\ -\sin \phi_{APP} \cos \theta_{APP} \\ -\cos \phi_{APP} \sin \theta_{APP} \end{pmatrix}_{BODY} = \begin{pmatrix} n_x \\ n_y \\ n_z \end{pmatrix} \quad [5]$$

$\theta_{APP}$  and  $\phi_{APP}$  can now be calculated as:

$$\theta_{APP} = \sin^{-1} \left( \frac{n_x}{|\vec{n}|} \right) \quad [6]$$

$$\phi_{APP} = \sin^{-1} \left( \frac{-n_y}{|\vec{n}| \cos \theta_{APP}} \right) \quad [7]$$

<sup>6</sup> Actually,  $\vec{n}$  has components  $\{0, 0, -1\}$ , since the load factor is normalized by the acceleration due to gravity ( $g$ ). However,  $\{0, 0, -g\}$  is used here to make it clear that the loads in the unaccelerated system are due to gravity.

The results of these calculations are shown in Figure 11. Note that throughout the flight, the “apparent” pitch angle ranged between  $0^\circ$  and  $15^\circ$ , and the “apparent” roll angle ranged between  $0^\circ$  and  $-4^\circ$ , even when the real pitch angle was as low as  $-42^\circ$  and the airplane was banked to the left as much as  $78^\circ$ . This suggests that even when the airplane was in a steeply banked descent, conditions were present that could have produced a somatogravic illusion of level flight.

## E. CONCLUSIONS

This *Aircraft Performance Radar & Simulation Study* presents the results of using Amarillo Airport Surveillance Radar (AMA ASR) data, evidence at the crash site, wind data derived from another aircraft, Air Traffic Control (ATC) communications, and simulation results to estimate the position and orientation of the airplane during the accident flight. The performance observations noted here are based on the results of the simulation described in detail in Section D-IV, which produces an airplane trajectory that closely matches the recorded radar data and crash site location.

After lifting off from KAMA runway 4, N933DC accelerated to about 193 KCAS while climbing between 600 and 1200 ft/min to an altitude of about 4400 ft above Mean Sea Level (MSL), or about 800 ft above ground level (AGL). The airplane leveled at 4300 to 4400 ft MSL until about 23:46:30, when it resumed climbing, reaching 6000 ft MSL (2400 ft AGL) at about 23:46:52. During this climb, the airplane decelerated from 193 KCAS to about 122 KCAS. At about 23:47:02, the airplane started an increasingly rapid descent from 6000 ft MSL to the ground (elevation 3600 ft MSL). The simulation rate of descent and airspeed at impact are about 17000 ft/min and 220 KCAS, respectively.

At about 23:45:42, while climbing through 4100 ft MSL (500 ft AGL), the airplane started a slow roll to the right, reaching a roll angle of about  $42^\circ$  at about 23:46:10. At 23:46:24 the roll angle had decreased to  $36^\circ$ , and the pitch angle started to increase steadily (consistent with the climb to 6000 ft MSL). At 23:46:32, when the roll angle was  $30^\circ$ , the airplane started rolling more quickly to the left, rolling through wings level at about 23:46:40 (then on a ground track of  $267^\circ$  true). The airplane achieved a peak pitch angle of about  $23^\circ$  at about 23:46:42, after which the pitch angle decreased steadily to an estimated  $-42^\circ$  at impact. As the pitch angle decreased, the roll angle increased steadily to the left, reaching an estimated  $-76^\circ$  at impact.

The simulation requires full throttle from 23:45:24 through 6000 ft MSL, except for two brief power reductions between 23:45:48 and 23:45:56 and between 23:46:28 and 23:46:30, when there is a pause in the increase in airspeed and the airplane levels briefly at 4400 MSL.

The simulation control inputs are well within the airplane’s control travel limits, and the computed column and wheel control forces required are generally (until the last 7 seconds of the flight) within the one-hand short-term force limit prescribed in 14 CFR paragraph §23.143. The simulation maximum normal load factor, reached at impact, was about 2.6 G’s. In addition, throughout the flight the simulation lift coefficient ( $C_L$ ) remained below the flaps-up maximum  $C_L$  ( $C_{Lmax}$ ) implied by the flaps-up stall speed published in the AFM, indicating that the airplane could fly the trajectory indicated by the radar data without stalling.

An estimate of the “apparent” pitch and roll angles, representing the attitude a pilot would “feel” the airplane to be in based on his vestibular / kinesthetic perception of the components of the load factor vector in his own body coordinate system, was made based on the simulation load

factors. The “apparent” pitch angle ranged between  $0^\circ$  and  $15^\circ$ , and the “apparent” roll angle ranged between  $0^\circ$  and  $-4^\circ$ , even when the real pitch angle was as low as  $-42^\circ$  and the airplane was banked to the left as much as  $78^\circ$ . This suggests that even when the airplane was in a steeply banked descent, conditions were present that could have produced a somatogravic illusion of level flight.

---

John O’Callaghan  
National Resource Specialist – Aircraft Performance  
Office of Research and Engineering

## F. REFERENCES

1. National Transportation Safety Board, *Preliminary Report, Pilatus Aircraft Ltd PC-12, Registration N933DC, Amarillo, TX, 04/28/2017 (NTSB Accident Number CEN17FA168)*. Available at: <https://app.nts.gov/pdfgenerator/ReportGeneratorFile.ashx?EventID=20170429X35104&AKey=1&RType=Prelim&IType=FA>
2. Pilatus Aircraft Ltd, *Pilot's Operating Handbook and FOCA Approved Airplane Flight Manual, PC-12 Series MSN 321, 401-544 and 546-888*, Pilatus Report # 02211, Issued March 30, 2001, Revision 4 issued April 30, 2007.
3. Federal Aviation Administration, *Aircraft Accident Package: AMA-ATCT-0396, LN933DC, PC12, April 29, 2017, 0448 UTC*.
4. Pilatus Aircraft Ltd., *Engineering Note Number EN 12-07-037, Control system data for the PC-12 simulator*, dated February 4, 1998.
5. Pilatus Aircraft Ltd., *Technical Memo TM-12-006107, PC-12 MSN 105 Accident – Trim Positions and Stick Pusher Cable Condition, Issue 1*, dated May 31, 2017.

# TABLES

Time, UTC (CDT)	Source	Content
04:46:11 (23:46:11)	AMA LC	med evac three delta Charlie reset transponder squawk four two six one
04:46:17 (23:46:17)	N933DC	uh sorry about that four two six one three delta charlie
04:46:33 (23:46:33)	AMA LC	i got you now contact departure y'all have a good night
04:46:37 (23:46:37)	N933DC	all right to departure three delta charlie
04:46:56 (23:46:56)	N933DC	and departure ah three delta charlie is with you uh six thousand
04:47:04 (23:47:04)	AMA WR1	med evac three delta charlie amarillo departure radar contact

**Table 1.** Air Traffic Control (ATC) communications with N933DC, from Reference 3. N933DC = accident airplane. AMA LC = Amarillo Air Traffic Control Tower Local Control Position. AMA WR1 = Amarillo West RADAR One Position.

Time, UTC (CDT)	Report Type	Wind	Visibility, statute miles	Sky Condition	Temperature / Dew Point, °C	Altimeter Setting, "Hg
03:53 (22:53)	METAR	010° @ 20 kt, gusting to 27 kt	10	600 ft AGL broken 3700 ft AGL overcast	08 / 07	29.77
04:53 (23:53)	METAR	360° @ 21 kt, gusting to 28 kt	10	700 ft AGL broken 1200 ft AGL overcast	07 / 07	29.78
05:42 (00:42)	SPECI	360° @ 16 kt, gusting to 28 kt	6 in light rain, mist	800 ft AGL broken 1400 ft AGL overcast	07 / 06	29.78

**Table 2.** Selected data from KAMA surface weather reports at times surrounding the accident.

Time CDT	Range nmi	Azimuth ACPs	Mode C pressure altitude, ft	North Latitude (computed)	West Longitude (computed)	Dist E of KAMA rwy 4, nmi	Dist N of KAMA rwy 4, nmi
23:45:01.1	0.45	3058	3800	35° 12" 58.01"	101° 43" 08.16"	0.6768	0.6589
23:45:06.1	0.39	3202	3800	35° 13" 02.61"	101° 43" 02.37"	0.7559	0.7355
23:45:11.2	0.36	3408	3800	35° 13" 07.99"	101° 42" 56.35"	0.8382	0.8249
23:45:16.3	0.38	3665	3900	35° 13" 14.62"	101° 42" 49.34"	0.9339	0.9354
23:45:21.5	0.42	3872	3900	35° 13" 19.54"	101° 42" 41.71"	1.0381	1.0173
23:45:26.4	0.52	4035	4000	35° 13" 26.03"	101° 42" 33.73"	1.1471	1.1253
23:45:31.4	0.62	60	4100	35° 13" 31.05"	101° 42" 25.07"	1.2653	1.2088
23:45:36.3	0.77	149	4200	35° 13" 37.92"	101° 42" 15.22"	1.3998	1.3232
23:45:41.2	0.91	218	4300	35° 13" 43.36"	101° 42" 05.13"	1.5375	1.4139
23:45:46.1	1.06	277	4400	35° 13" 48.49"	101° 41" 54.07"	1.6887	1.4992
23:45:51.1	1.22	336	4400	35° 13" 52.84"	101° 41" 41.17"	1.8647	1.5717
23:45:55.9	1.36	406	4600	35° 13" 53.72"	101° 41" 26.93"	2.0592	1.5865
23:46:00.9	1.48	489	4600	35° 13" 50.65"	101° 41" 11.52"	2.2697	1.5355
23:46:05.9	1.58	588	4600	35° 13" 42.62"	101° 40" 55.86"	2.4836	1.4020
23:46:10.7	1.62	700	4600	35° 13" 28.78"	101° 40" 44.62"	2.6372	1.1718
23:46:15.8	1.61	822	4600	35° 13" 11.16"	101° 40" 39.58"	2.7062	0.8785

**Table 3a.** AMA ASR returns for beacon code 4254. Latitude, longitude, north, and east values are computed from recorded range and azimuth.

Time CDT	Range nmi	Azimuth ACPs	Mode C pressure altitude, ft	North Latitude (computed)	West Longitude (computed)	Dist E of KAMA rwy 4, nmi	Dist N of KAMA rwy 4, nmi
23:46:20.7	1.52	953	4500	35° 12" 52.02"	101° 40" 44.47"	2.6396	0.5598
23:46:25.8	1.36	1081	4500	35° 12" 36.47"	101° 40" 58.71"	2.4452	0.3009
23:46:30.6	1.14	1195	4600	35° 12" 28.16"	101° 41" 19.04"	2.1675	0.1624
23:46:35.6	0.94	1297	5000	35° 12" 25.44"	101° 41" 38.17"	1.9063	0.1171
23:46:40.6	0.8	1422	5600	35° 12" 24.07"	101° 41" 55.27"	1.6728	0.0943
23:46:45.7	0.73	1613	5900	35° 12" 20.91"	101° 42" 11.40"	1.4525	0.0416
23:46:50.7	0.78	1832	6200	35° 12" 14.49"	101° 42" 25.94"	1.2539	-0.0654
23:46:55.8	0.92	1969	6200	35° 12" 04.36"	101° 42" 36.61"	1.1081	-0.2340
23:47:00.6	1.12	2002	6200	35° 11" 51.57"	101° 42" 40.81"	1.0508	-0.4469
23:47:05.4	1.3	1965	6100	35° 11" 39.76"	101° 42" 36.61"	1.1083	-0.6435
23:47:10.2	1.39	1882	5700	35° 11" 33.73"	101° 42" 24.07"	1.2796	-0.7438
23:47:14.8	1.28	1801	4900	35° 11" 40.71"	101° 42" 13.45"	1.4246	-0.6276

**Table 3b.** AMA ASR returns for beacon code 4261. Latitude, longitude, north, and east values are computed from recorded range and azimuth.

Item	Weight, lb	Arm, in	Moment, lb-in
Empty	6478.1	232.53	1506352.593
Pilot	230	160.27	36862.1
Co-pilot	0	160.27	0
Seat 1	190	236	44840
Seat 2	0	236	0
Seat 3	0	269	0
Patient	0	277	0
Seat 5	230	344	79120
Aft Bag	200	361	72200
<b>Zero Fuel Weight</b>	<b>7328.1</b>	<b>237.4</b>	<b>1739374.693</b>
Fuel	2000	232.373	464746
<b>Total TOW</b>	<b>9328.1</b>	<b>236.3</b>	<b>2204120.693</b>
LEMAC <sup>7</sup>	17.67 ft		
MAC <sup>8</sup>	5.6102 ft		
<b>CG % MAC</b>	<b>36.02%</b>		

**Table 4.** Weight and balance calculation based on information provided by Rico Aviation.

Item	Value
Vertical CG position	1.18 ft above reference plane (cabin floor)
Lateral CG position	on centerline
Ixx (slugs-ft <sup>2</sup> )	15000
Iyy (slugs-ft <sup>2</sup> )	20000
Izz (slugs-ft <sup>2</sup> )	29000
Ixz (slugs-ft <sup>2</sup> )	1330

**Table 5.** Additional mass properties information used in the simulation of the accident flight.

<sup>7</sup> LEMAC = Fuselage station of the leading edge of the mean aerodynamic chord.

<sup>8</sup> MAC = mean aerodynamic chord.

# FIGURES

# CEN17FA168: Pilatus PC-12, N933DC, Amarillo, TX, 04/28/2017

## Plan view of radar data and simulation trajectory

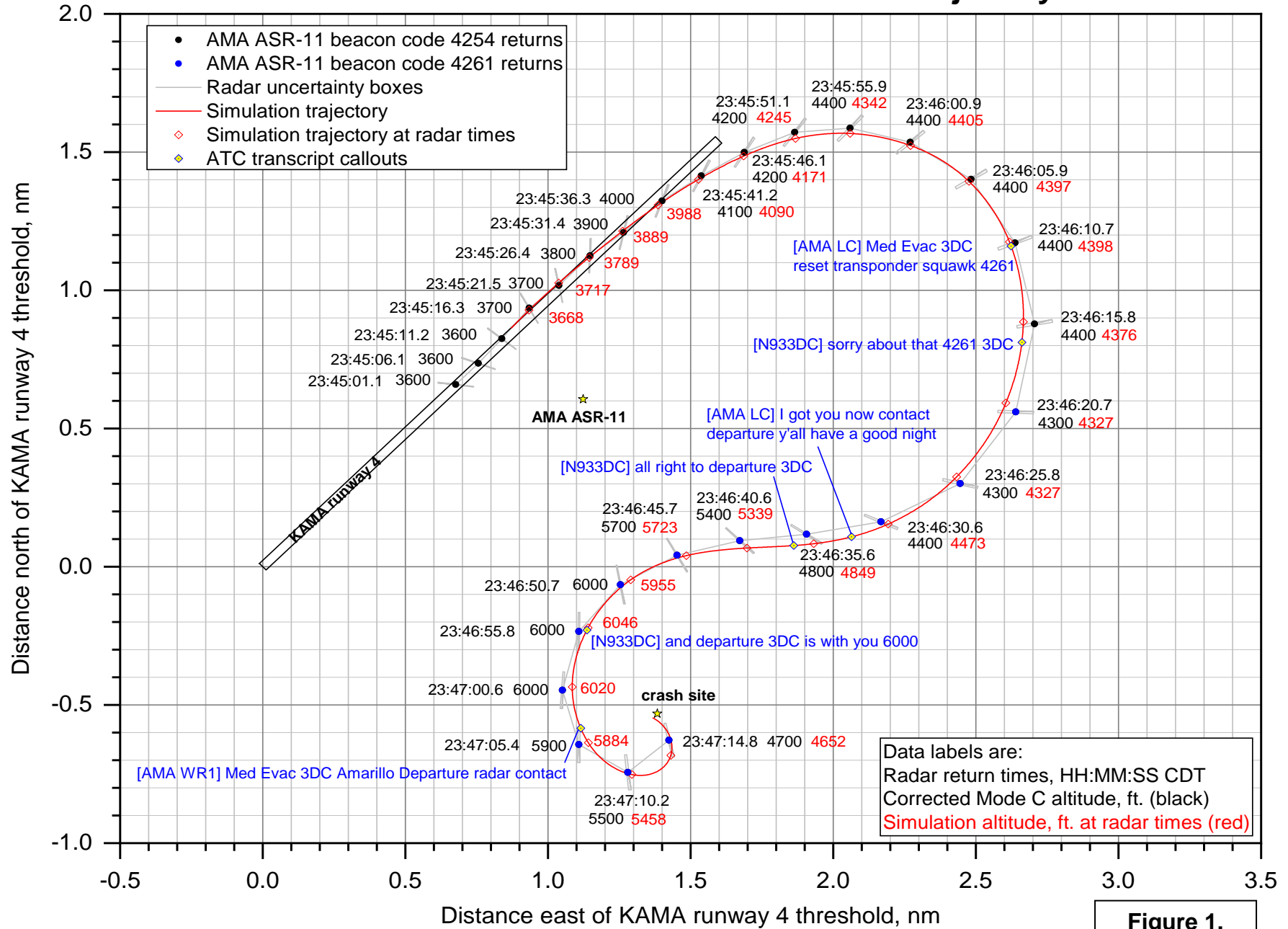
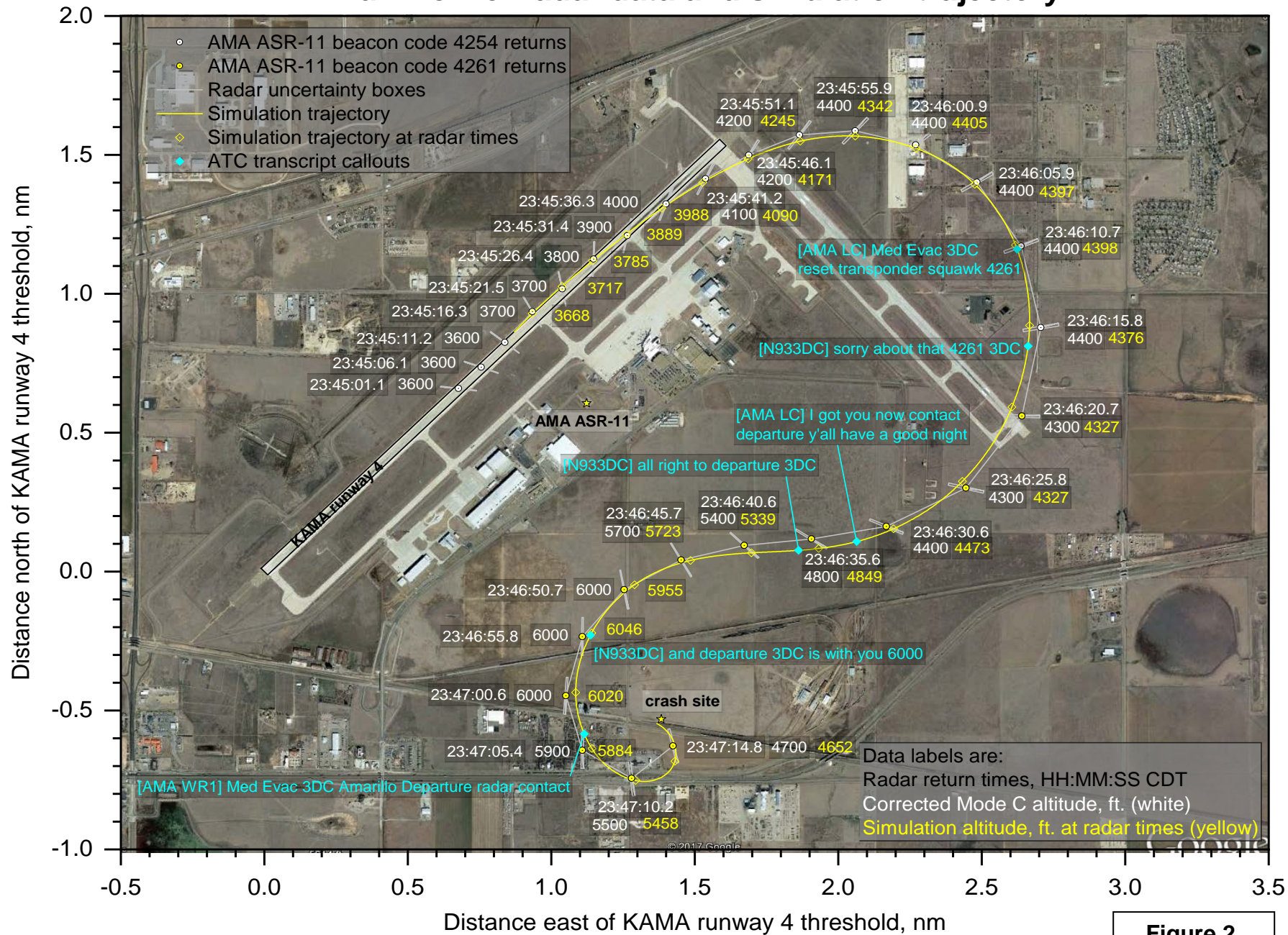


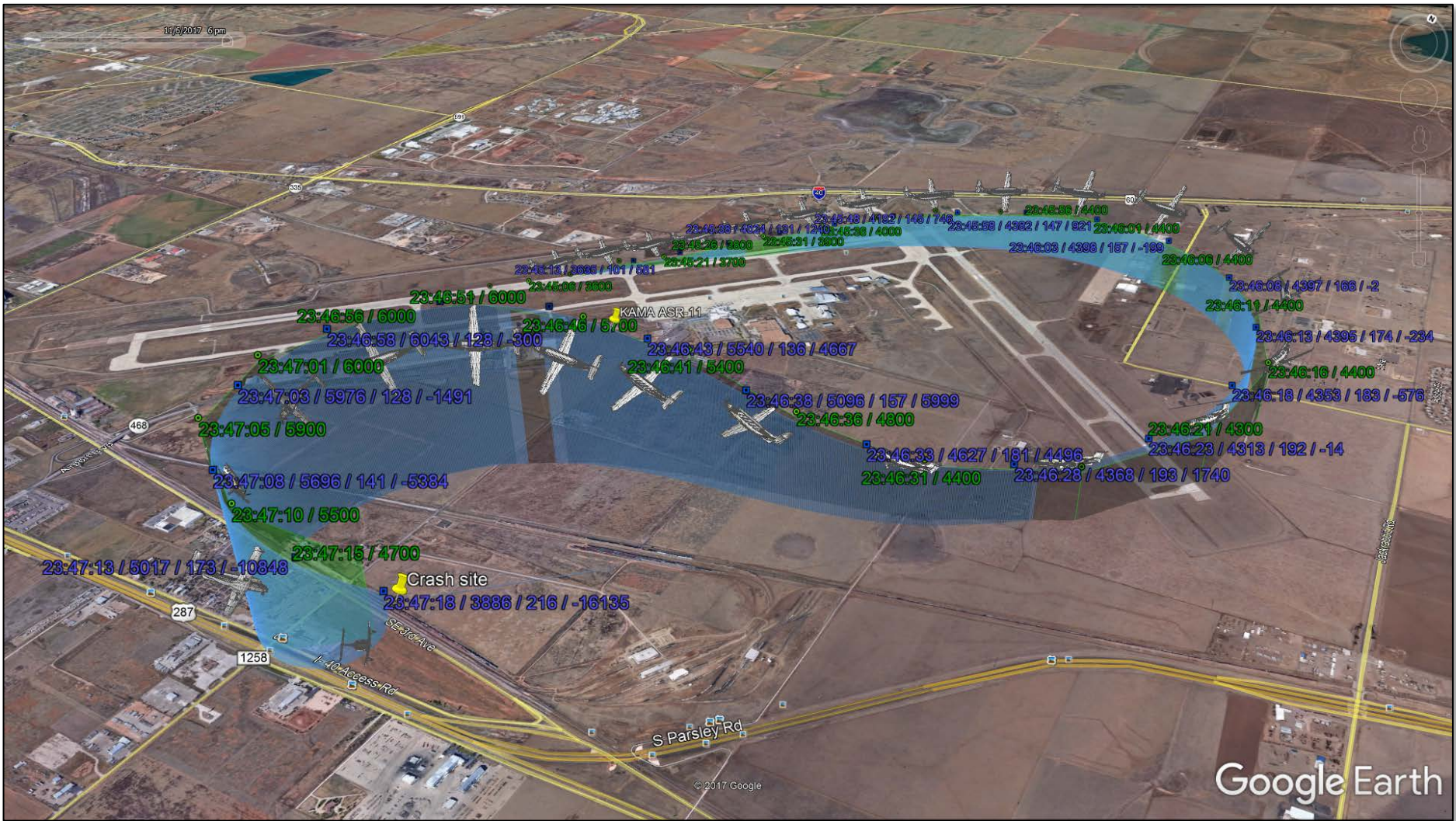
Figure 1.

# CEN17FA168: Pilatus PC-12, N933DC, Amarillo, TX, 04/28/2017

## Plan view of radar data and simulation trajectory



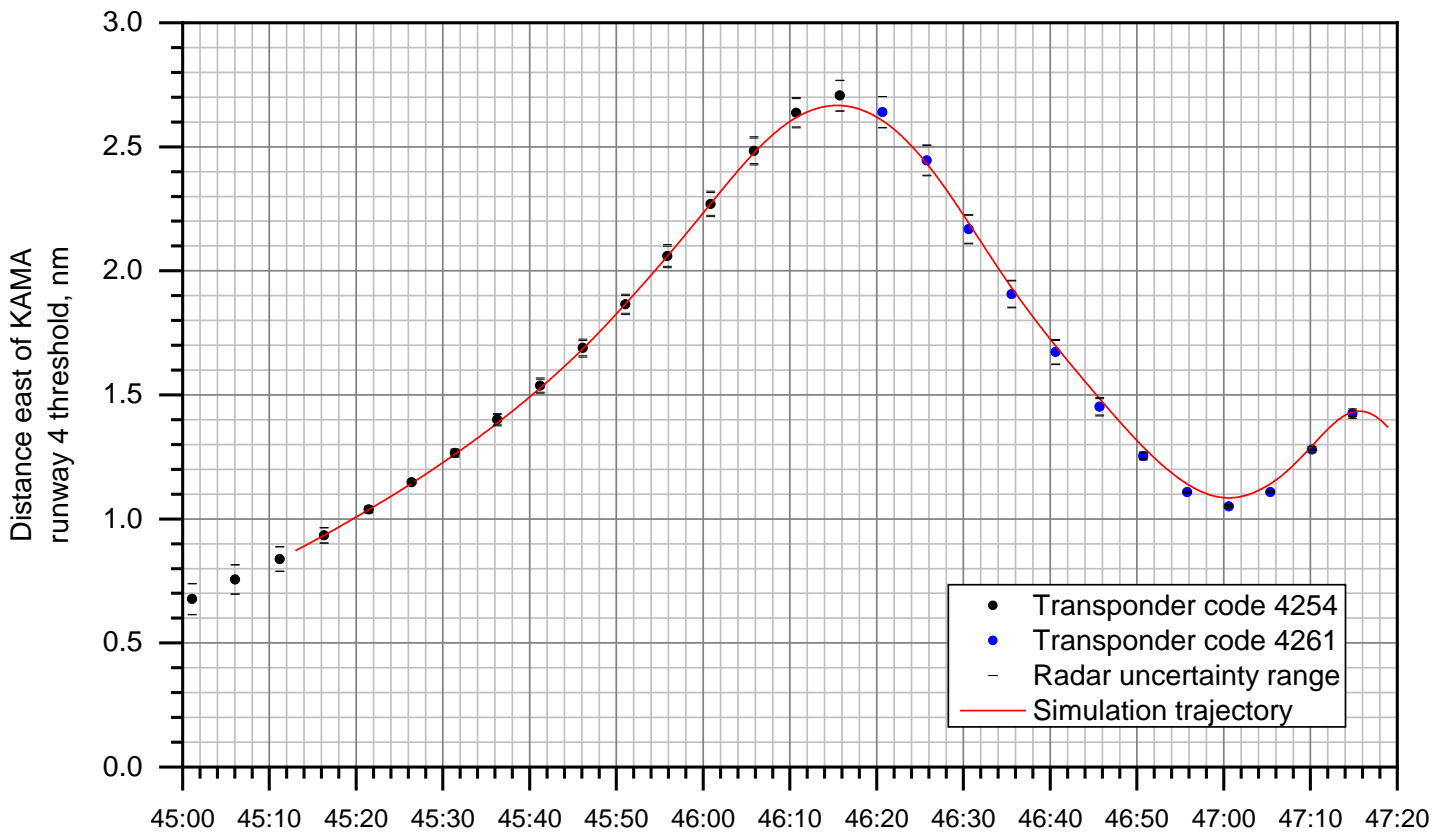
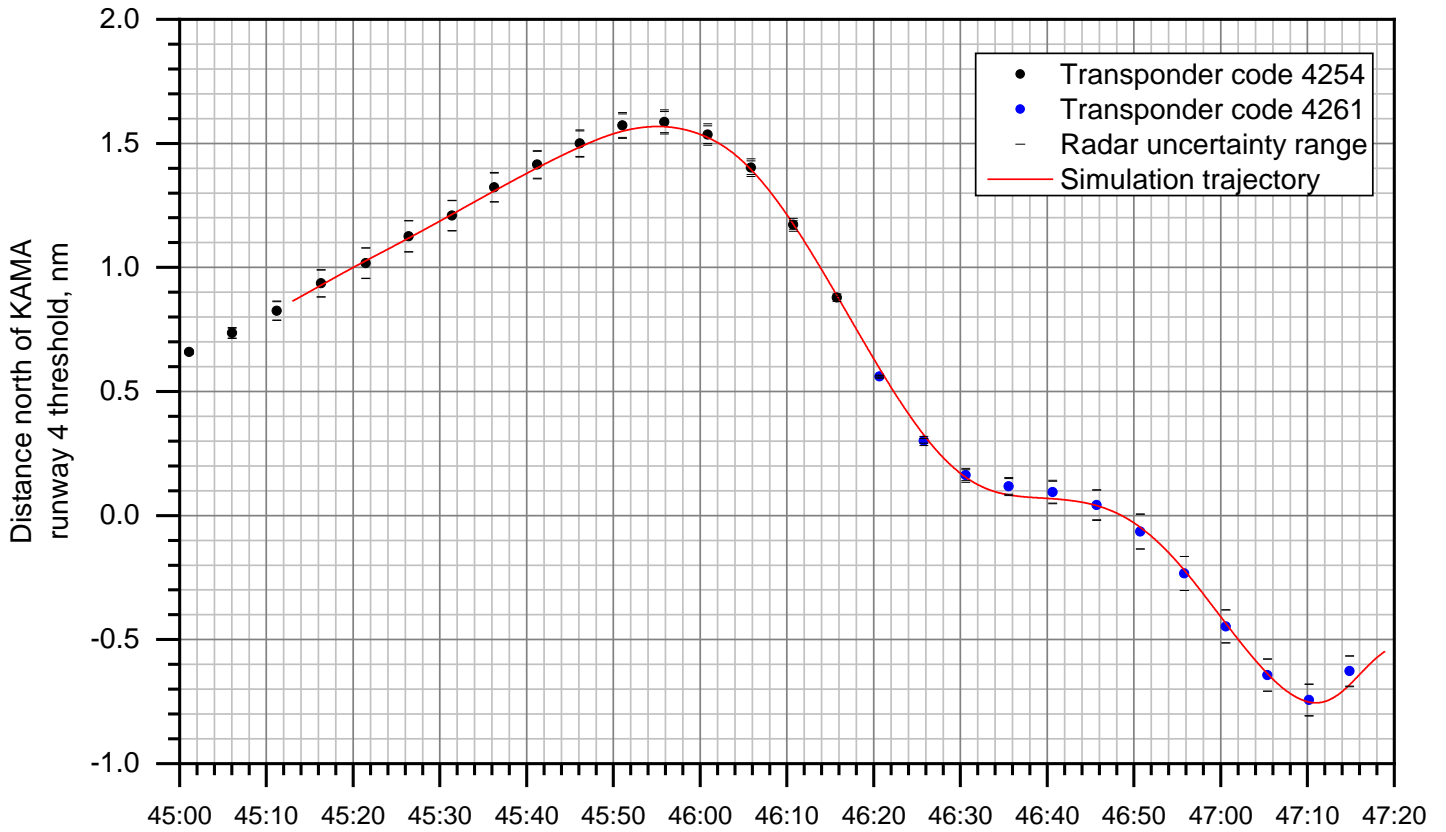
**Figure 2.**



**NOTE:** Airplane figures are drawn larger than their correct proportions for greater visibility. Green labels are AMA ASR data (time CDT / altitude ft MSL); blue labels are simulation data (time CDT / altitude ft MSL / speed KCAS / rate of climb ft/min).

**Figure 3.**

Radar & simulation north & east coordiantes vs. time



AMA ASR-11 time, MM:SS after 23:00:00 CDT

Figure 4.

# CEN17FA168: Pilatus PC-12, N933DC, Amarillo, TX, 04/28/2017

## Mode C and simulation altitudes vs. time

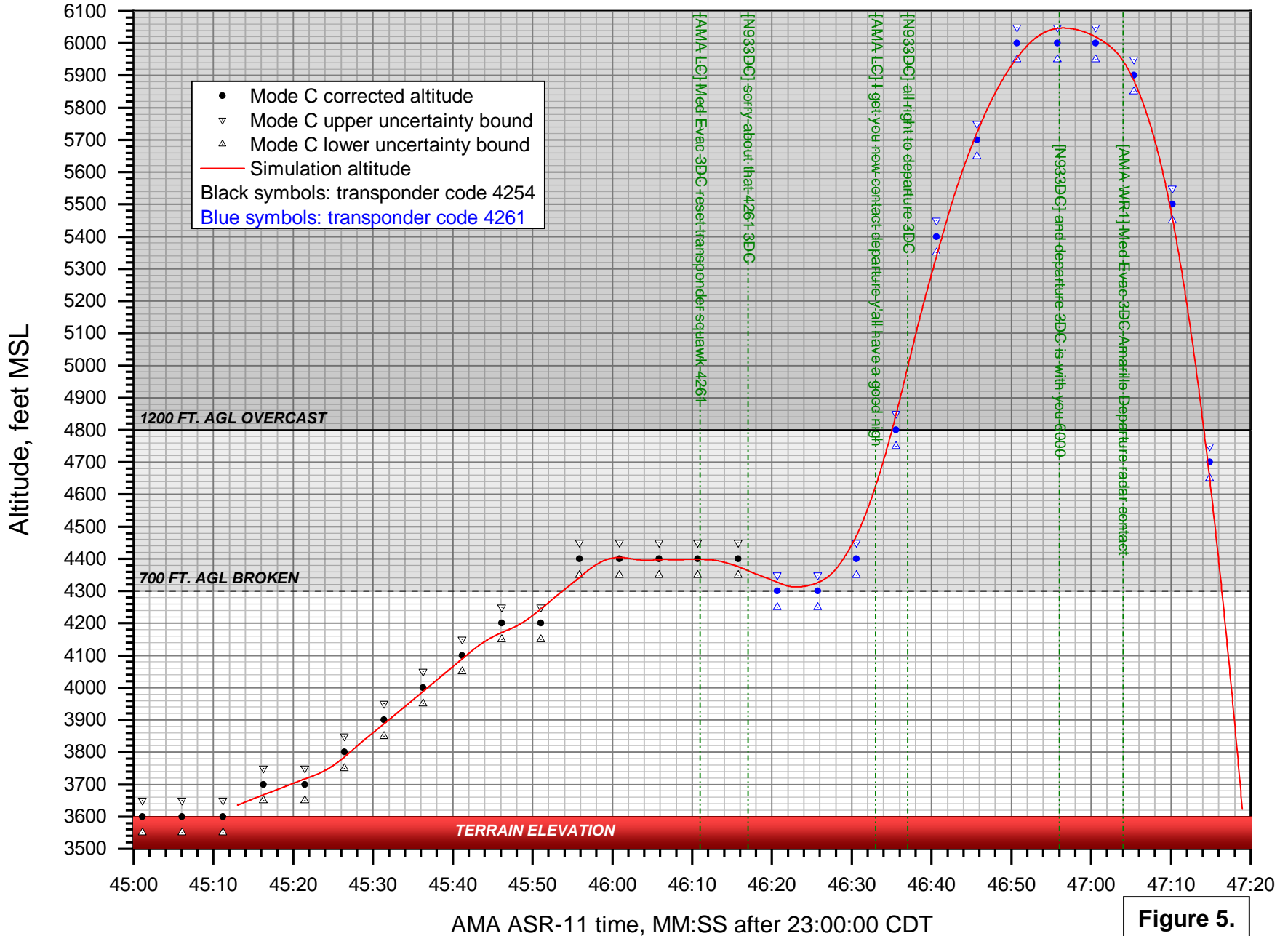


Figure 5.



Figure 6. Photograph of crash scene, from Reference 1. Arrow depicts direction of north.



(a)



(b)

Figure 7. Stills from video of accident scene. Arrow depicts direction of north.

# CEN17FA168: Pilatus PC-12 N933DC, Amarillo, TX, 4/28/2017

## Winds aloft from Boeing 737 FDR data

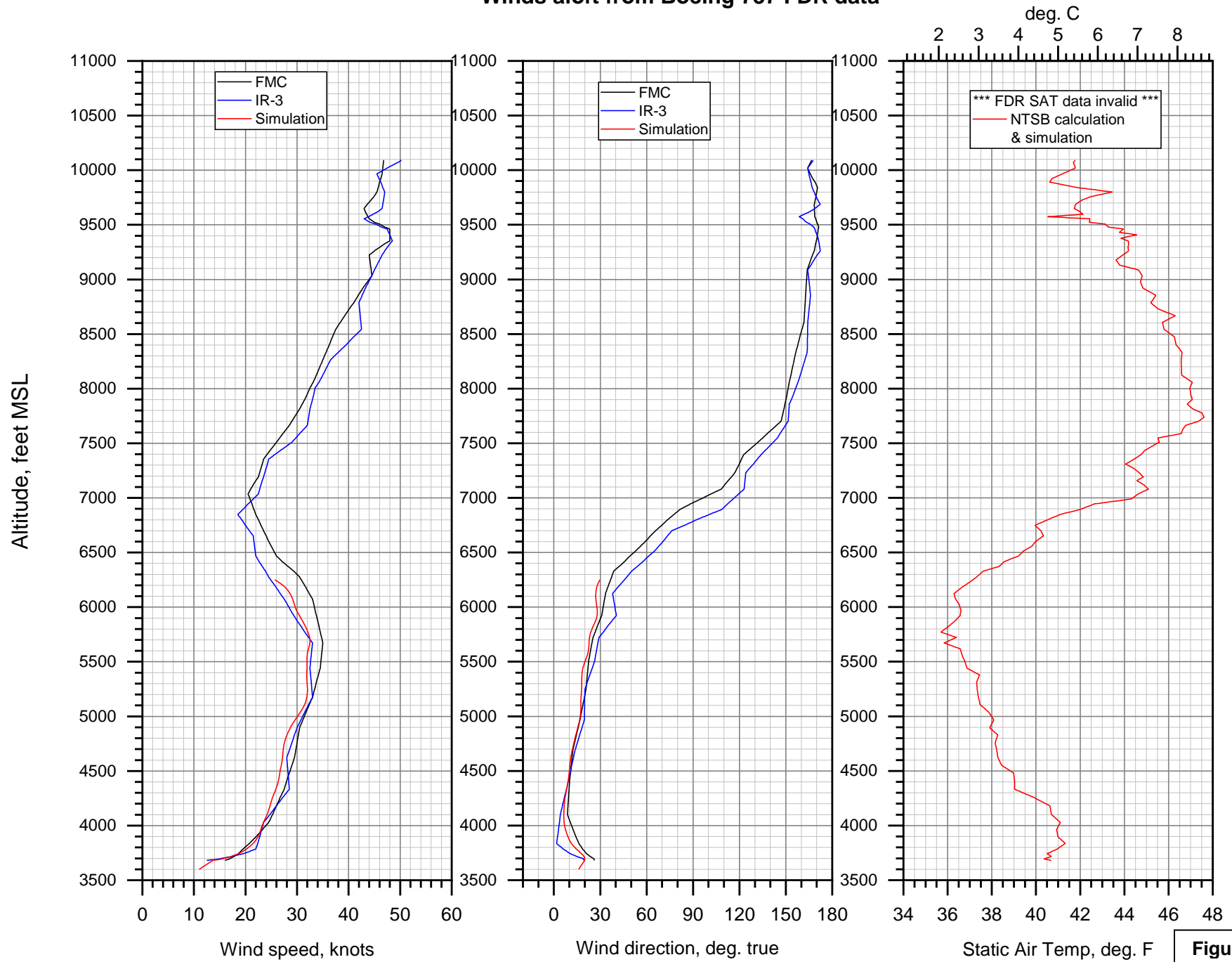


**Figure 8.**

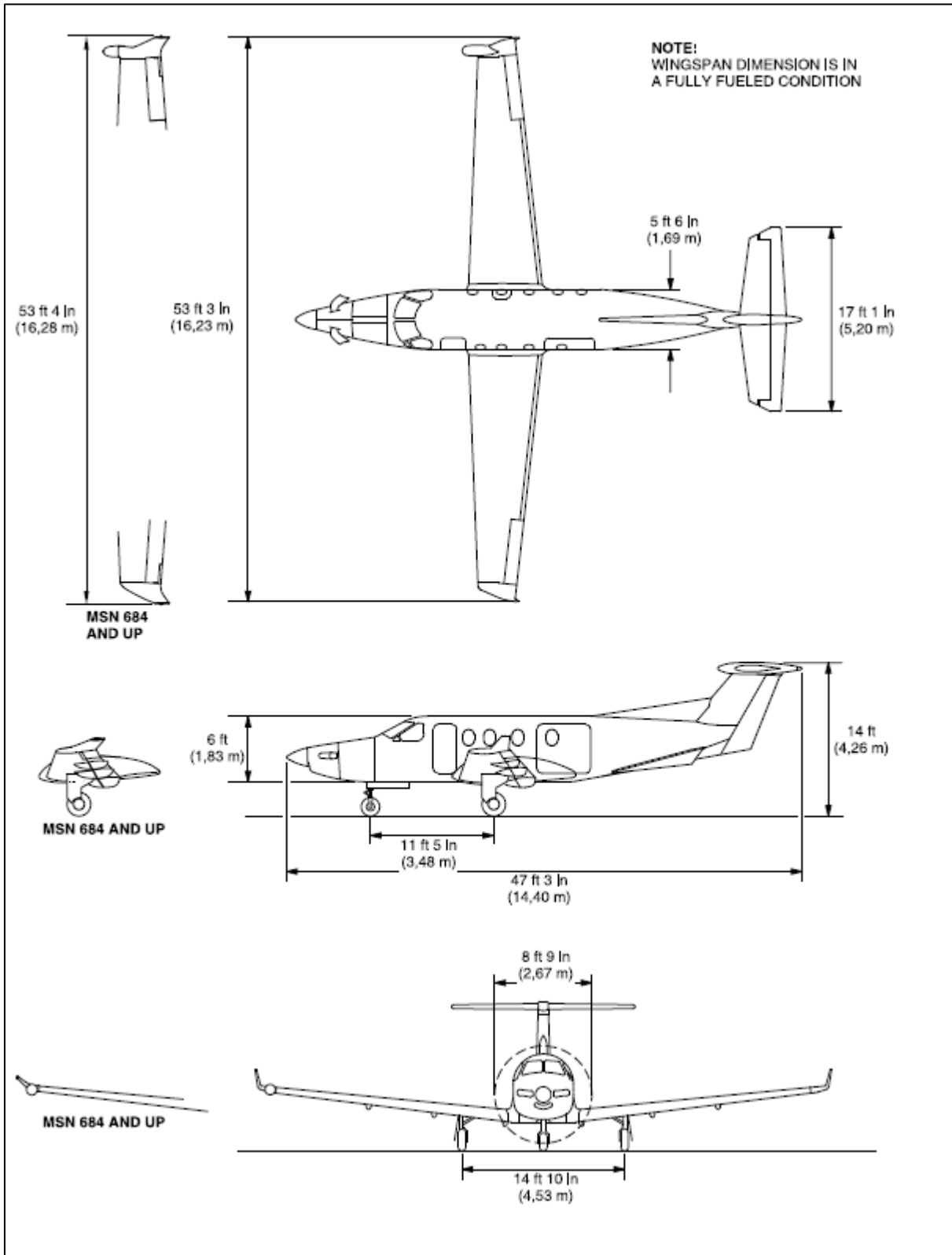
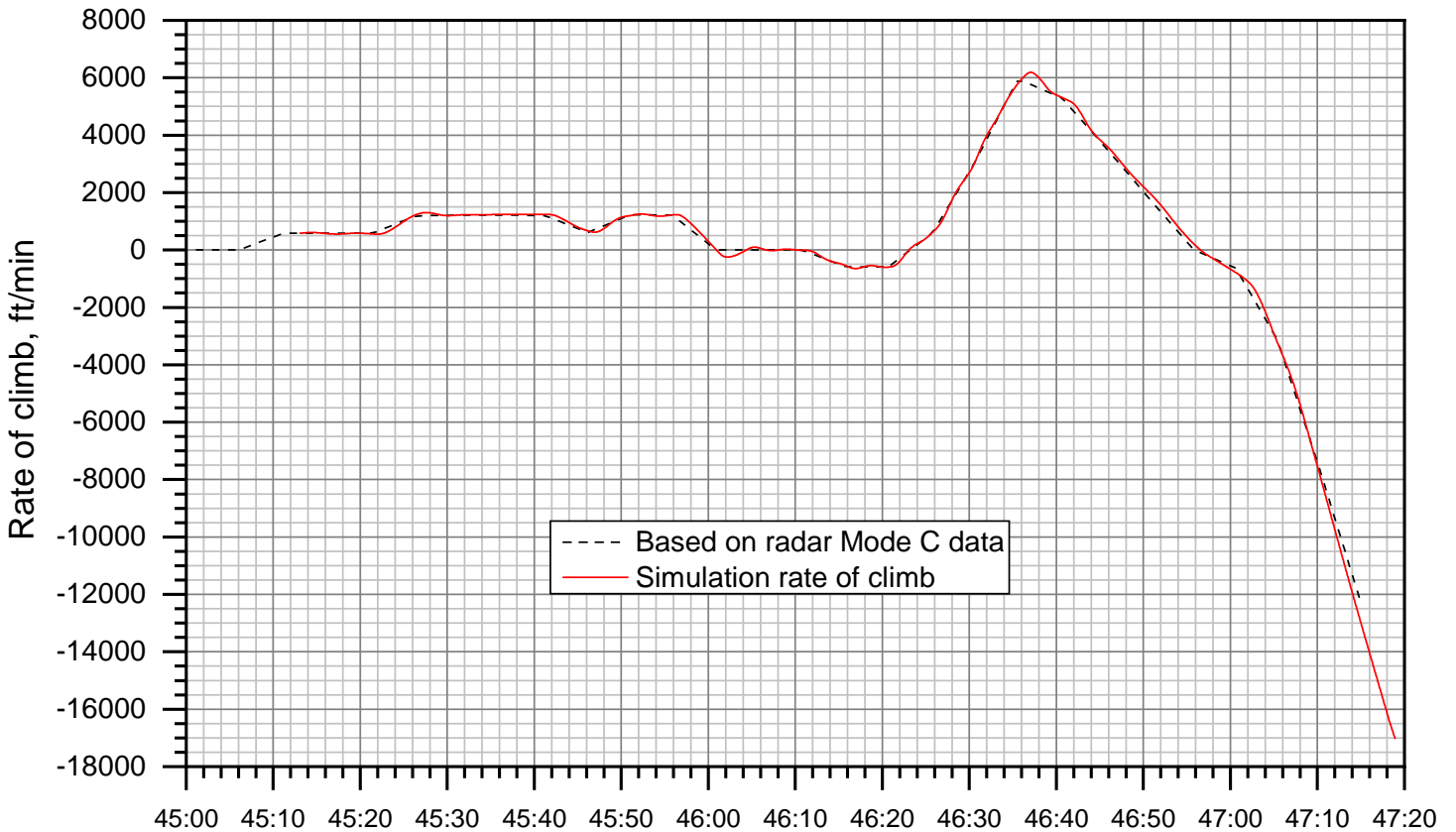
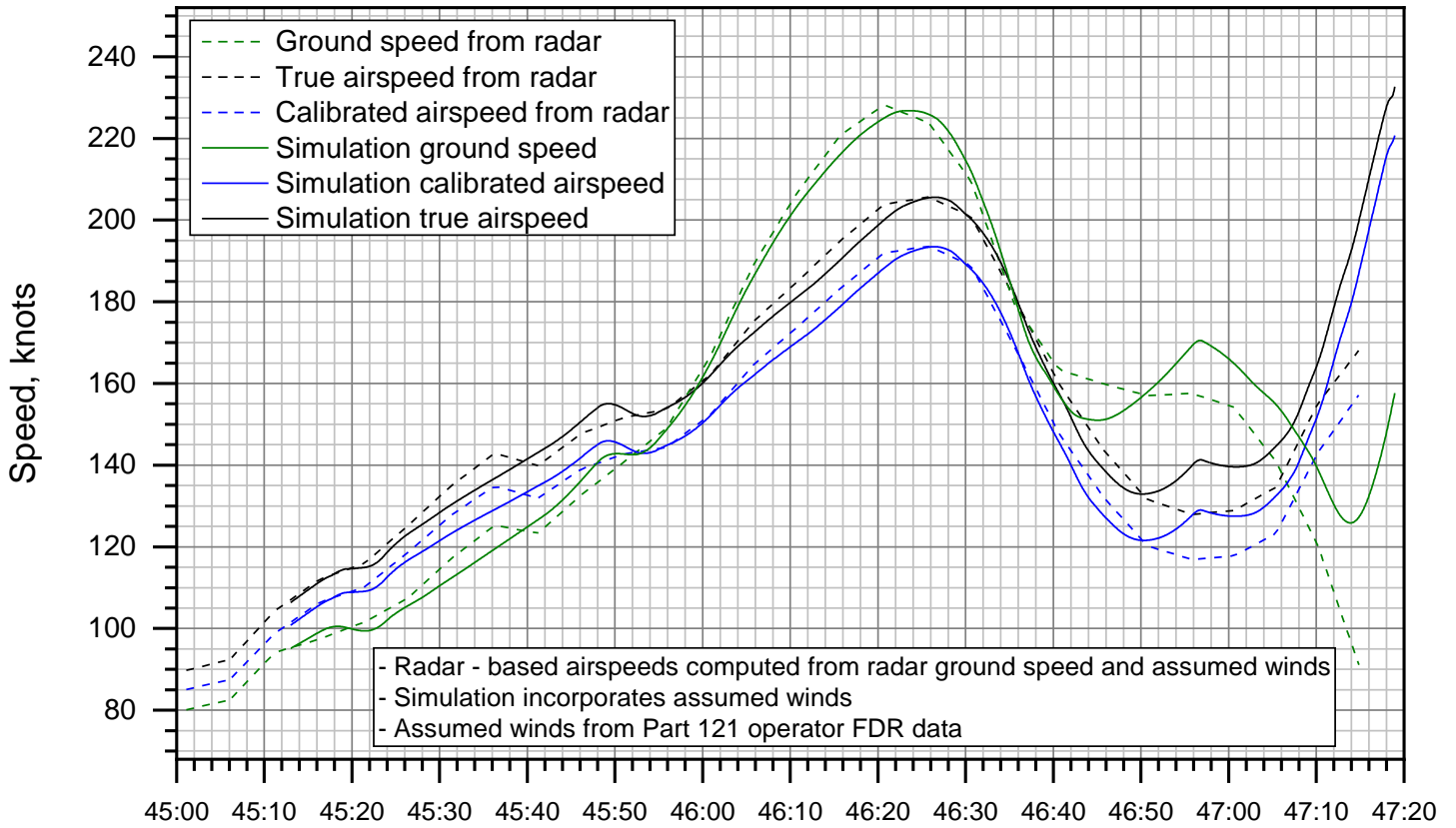


**Figure 9.** AFM 3-view drawing of the Pilatus PC-12 (from Reference 2).

# CEN17FA168: Pilatus PC-12, N933DC, Amarillo, TX, 04/28/2017

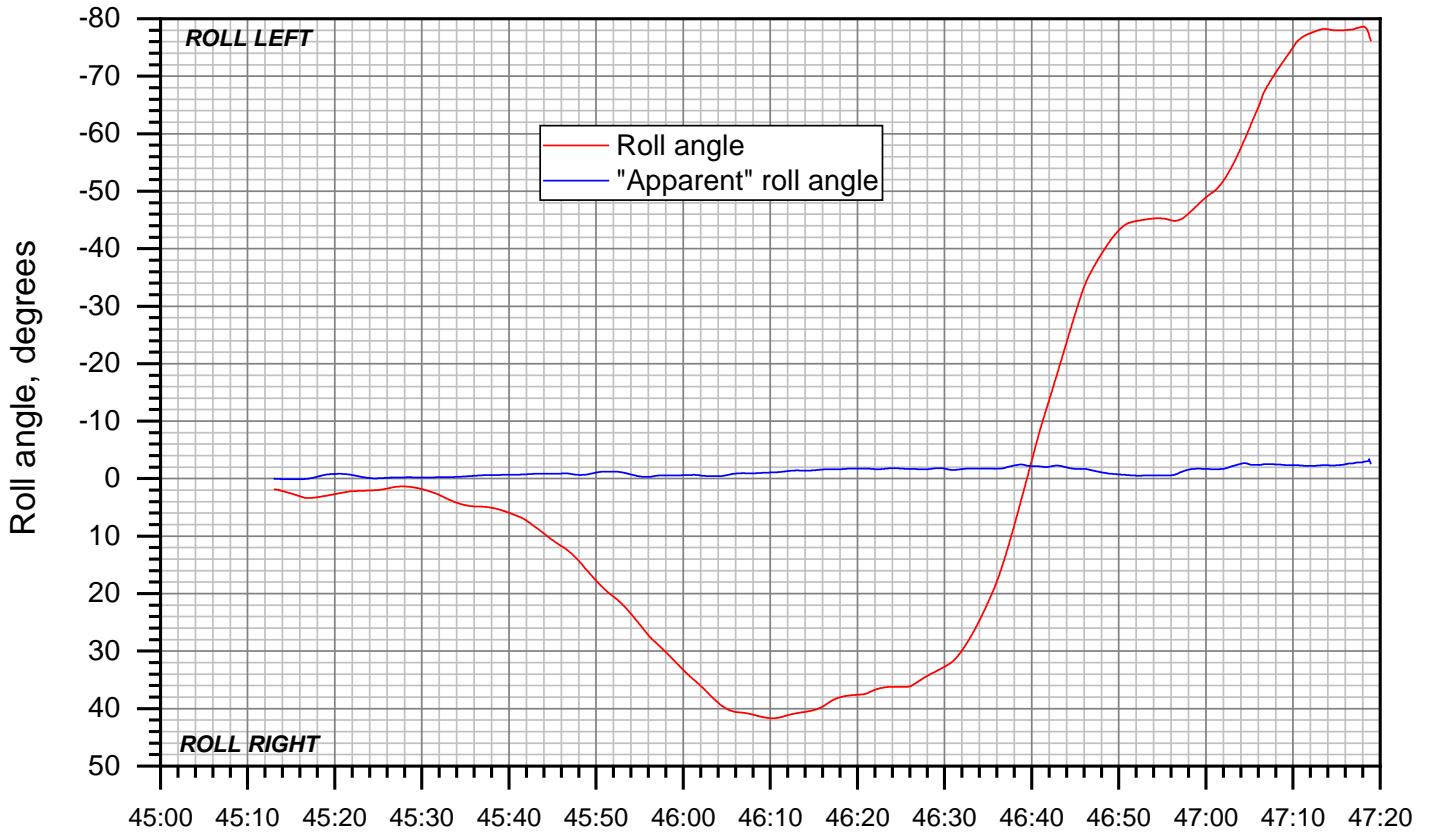
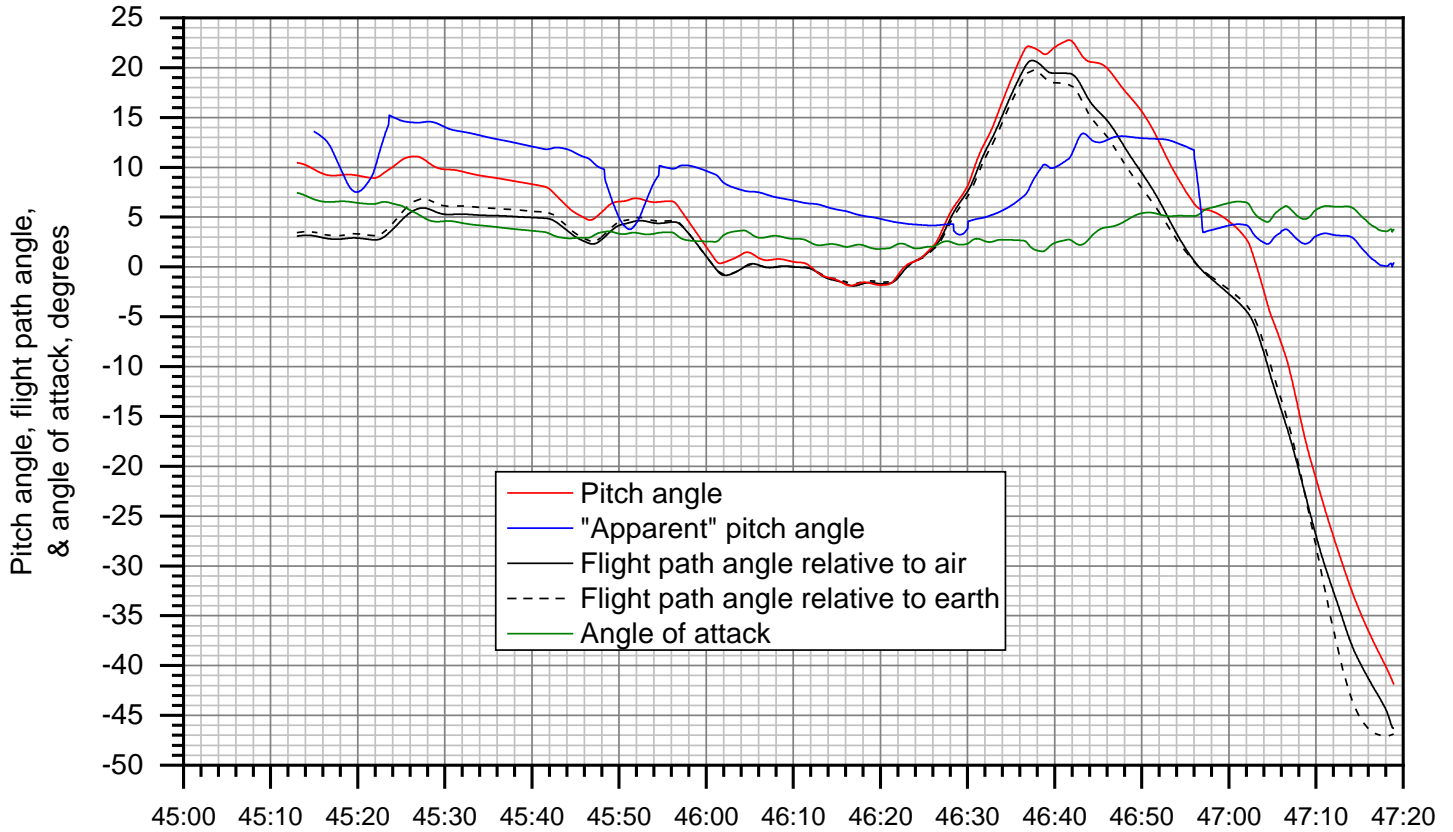
## Speeds and rate of climb



AMA ASR-11 time, MM:SS after 23:00:00 CDT

**Figure 10.**

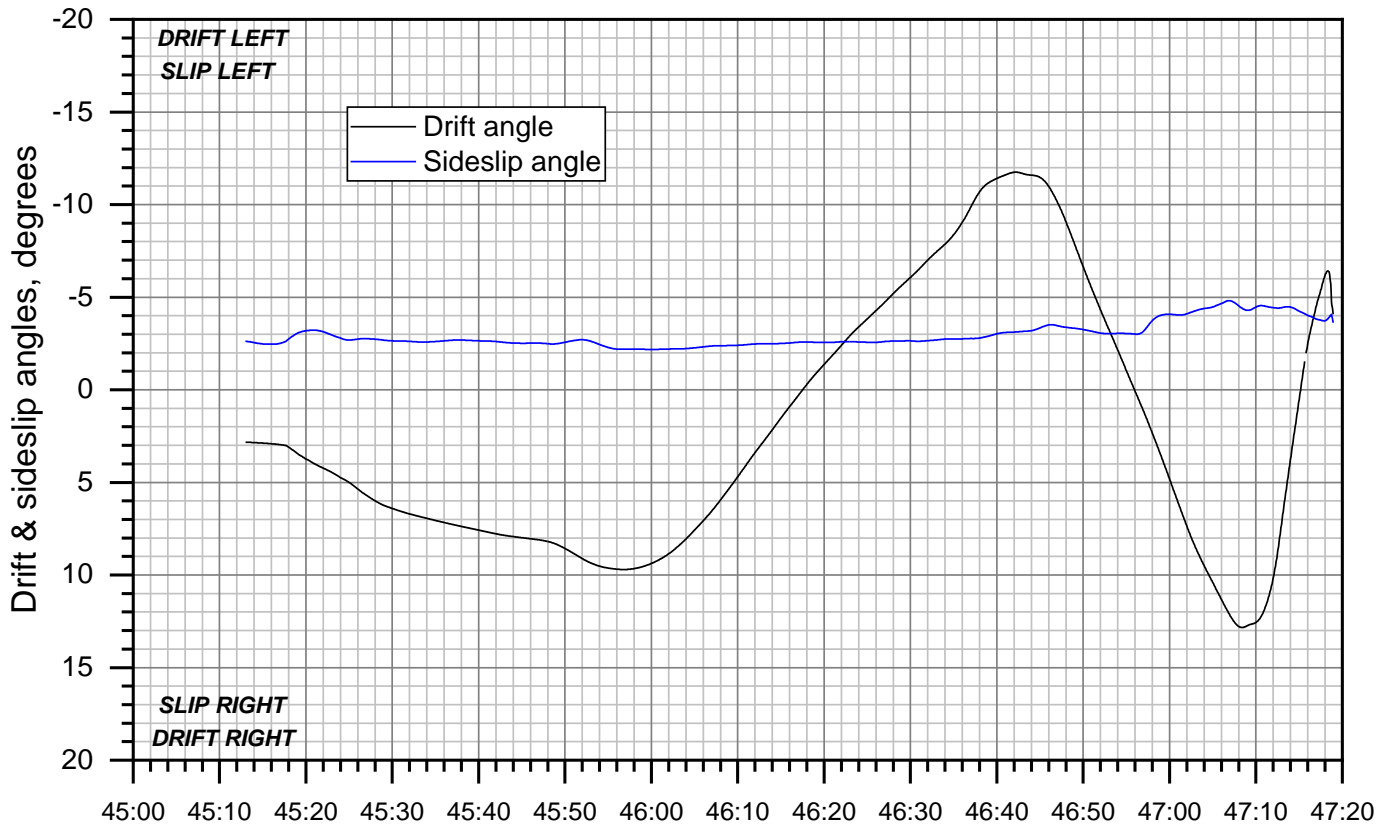
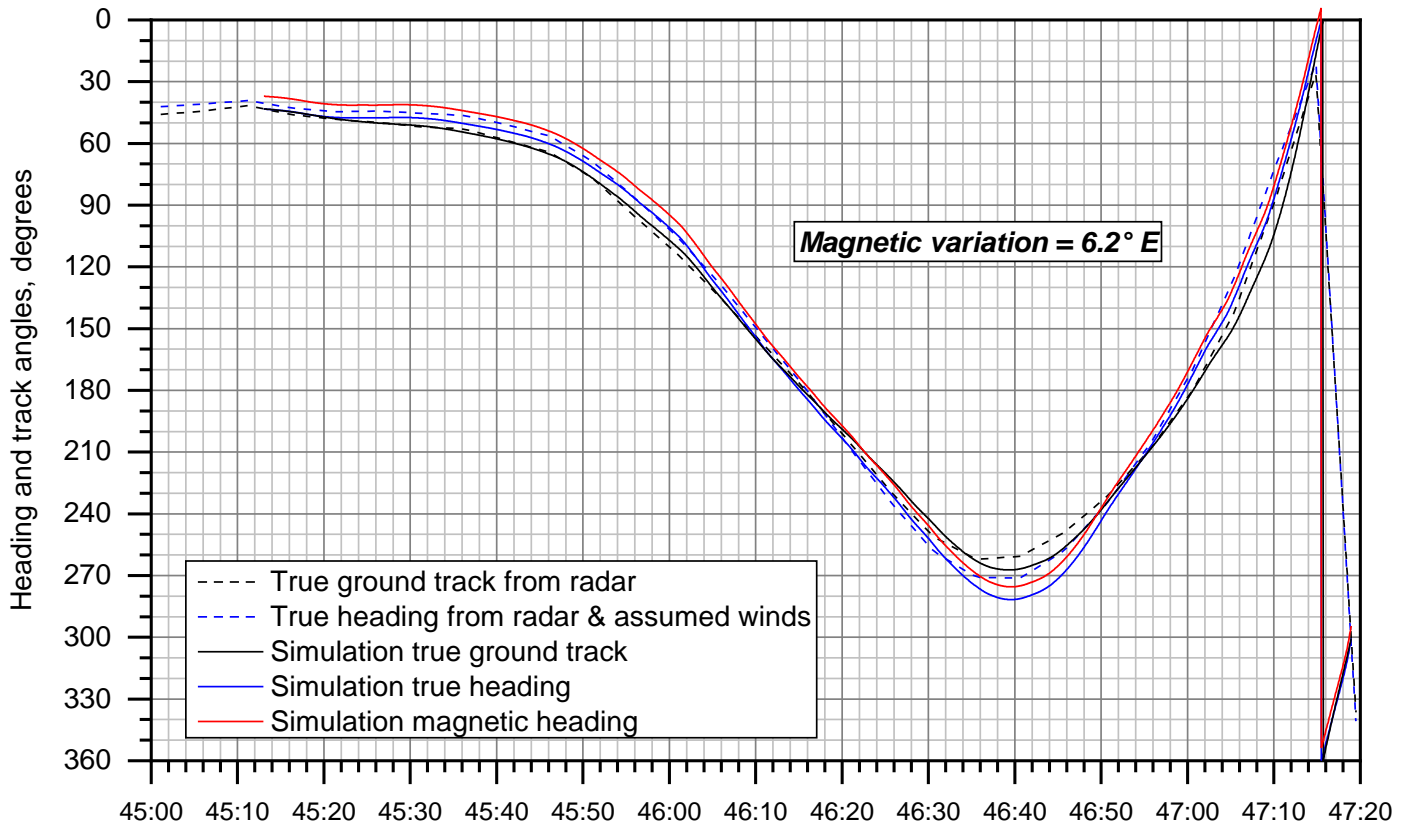
Simulation pitch & roll angles



AMA ASR-11 time, MM:SS after 23:00:00 CDT

Figure 11.

Heading, track, and drift angles

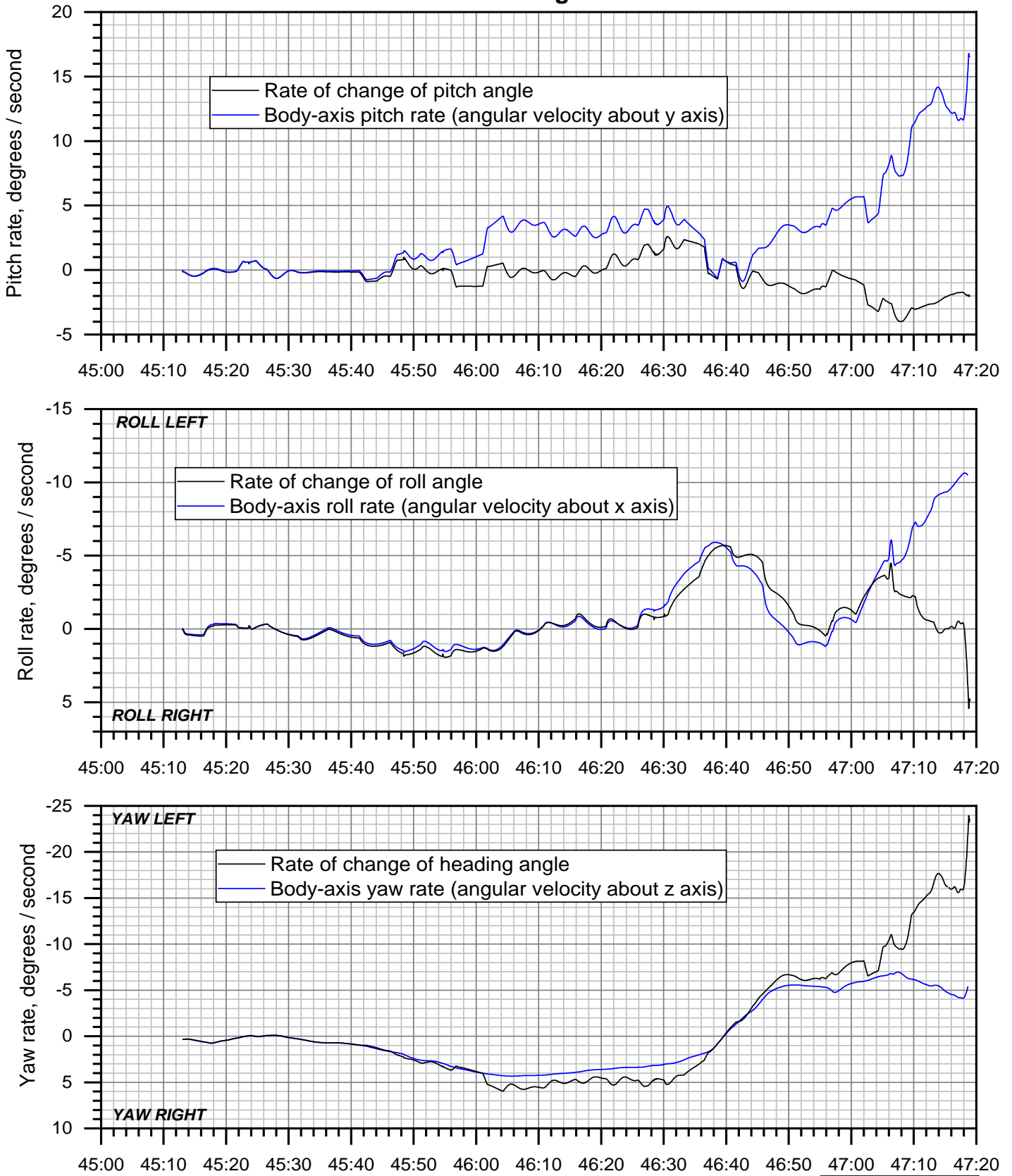


AMA ASR-11 time, MM:SS after 23:00:00 CDT

Figure 12.

# CEN17FA168: Pilatus PC-12, N933DC, Amarillo, TX, 04/28/2017

## Simulation angular rates

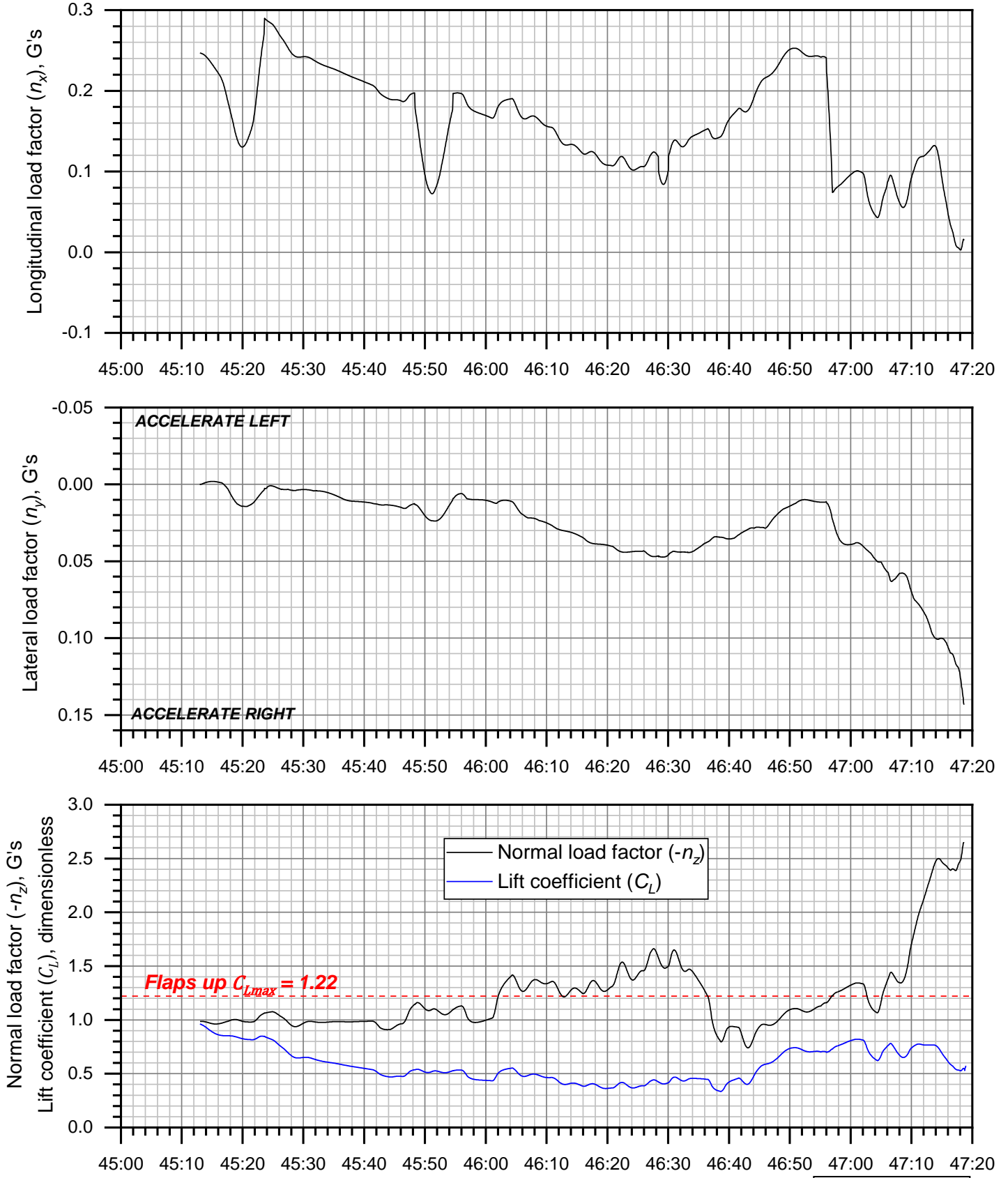


AMA ASR-11 time, MM:SS after 23:00:00 CDT

**Figure 13.**

# CEN17FA168: Pilatus PC-12, N933DC, Amarillo, TX, 04/28/2017

## Simulation load factors & lift coefficient

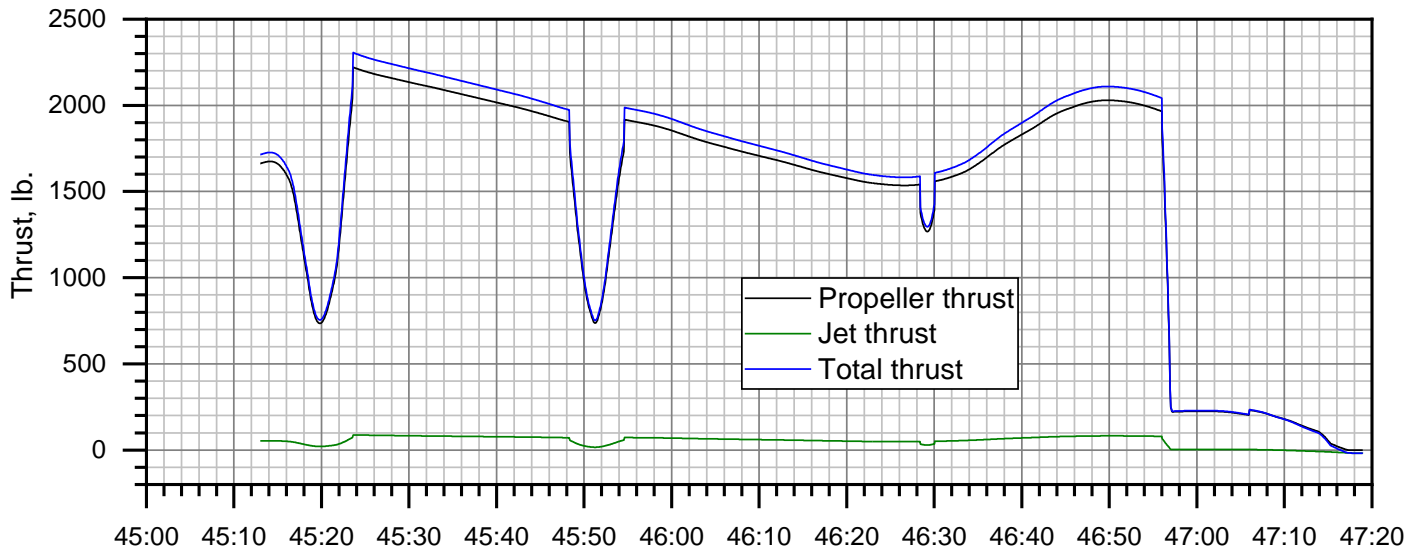
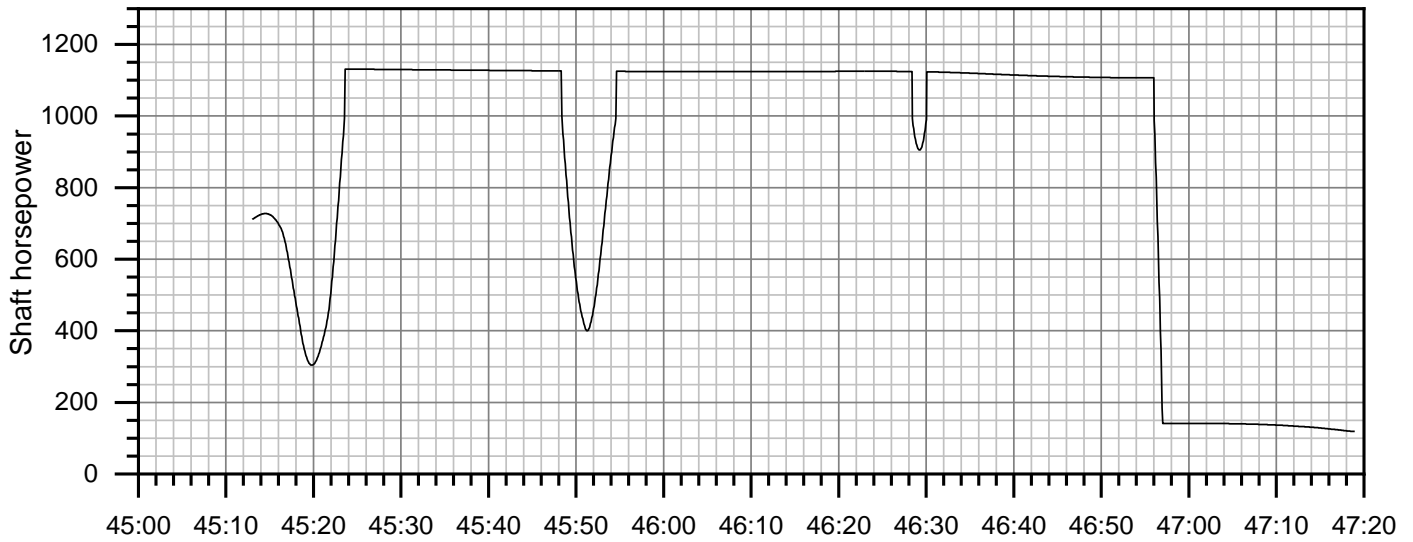
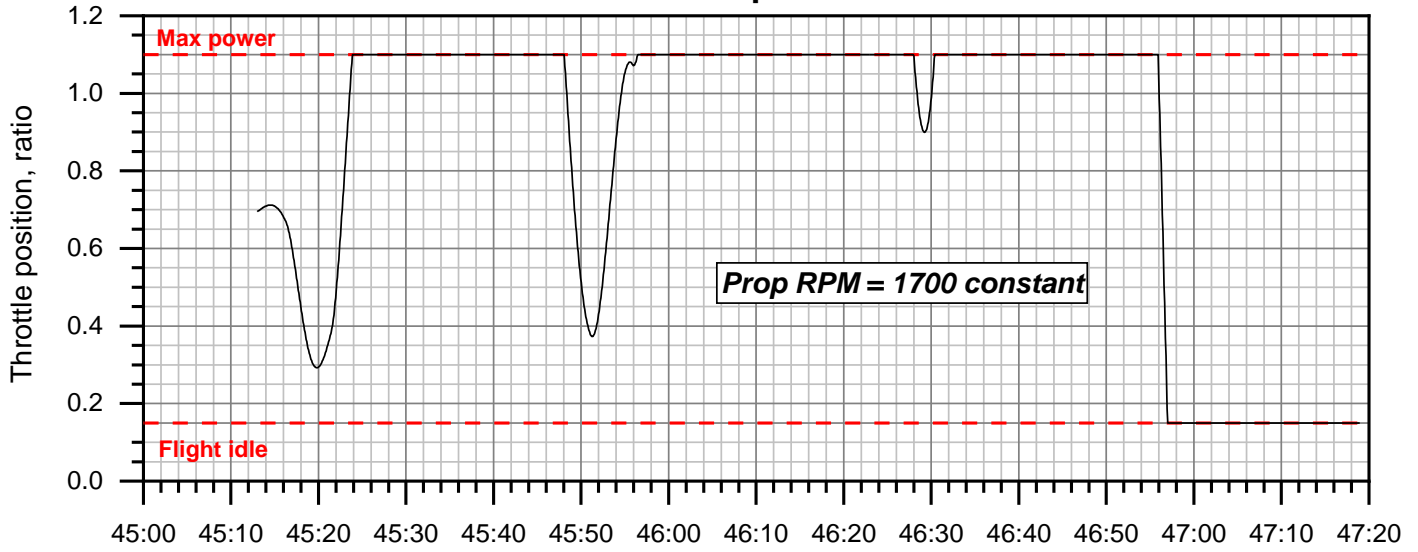


AMA ASR-11 time, MM:SS after 23:00:00 CDT

Figure 14.

# CEN17FA168: Pilatus PC-12, N933DC, Amarillo, TX, 04/28/2017

## Simulation power and thrust

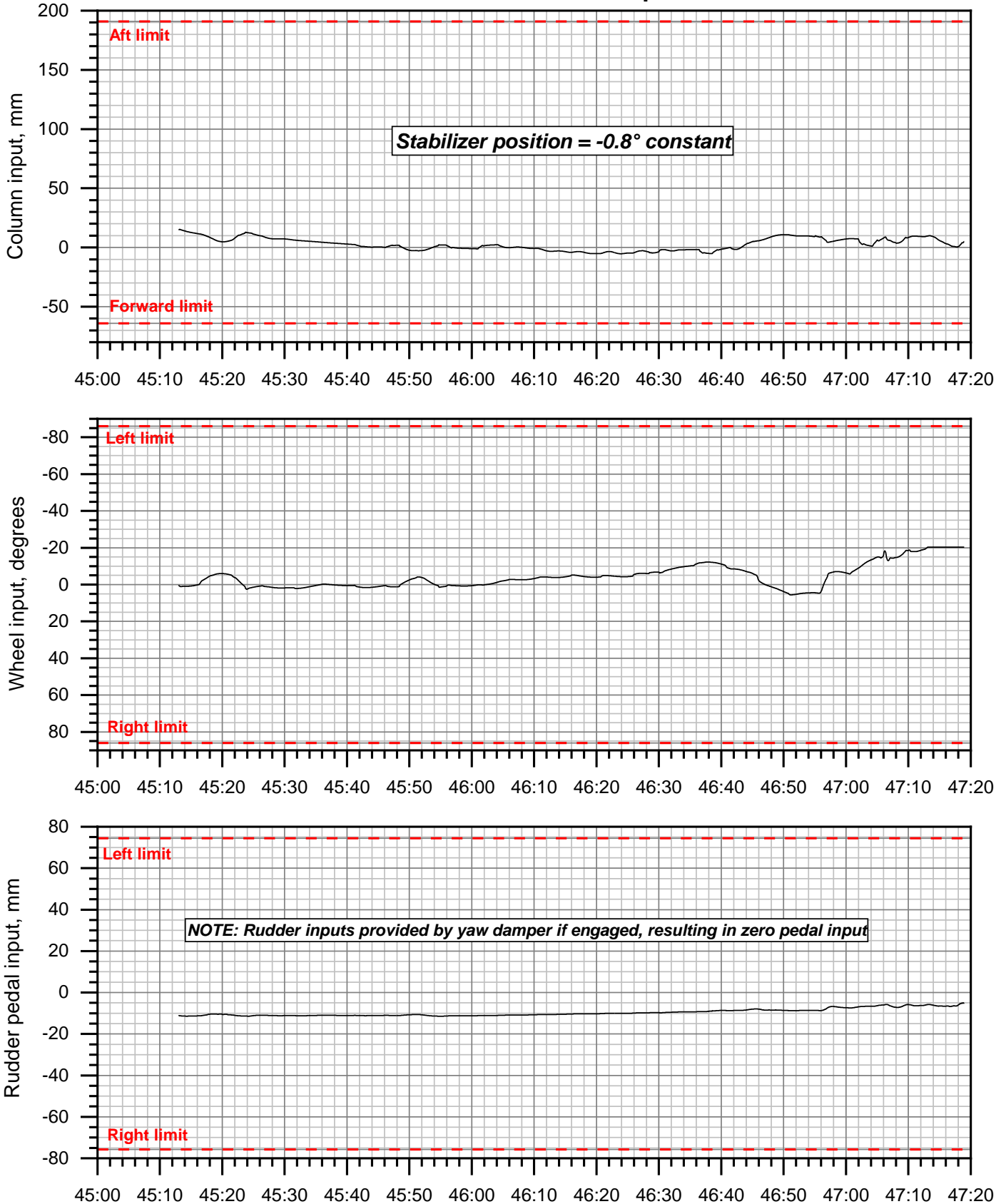


AMA ASR-11 time, MM:SS after 23:00:00 CDT

Figure 15.

# CEN17FA168: Pilatus PC-12, N933DC, Amarillo, TX, 04/28/2017

## Simulation control inputs

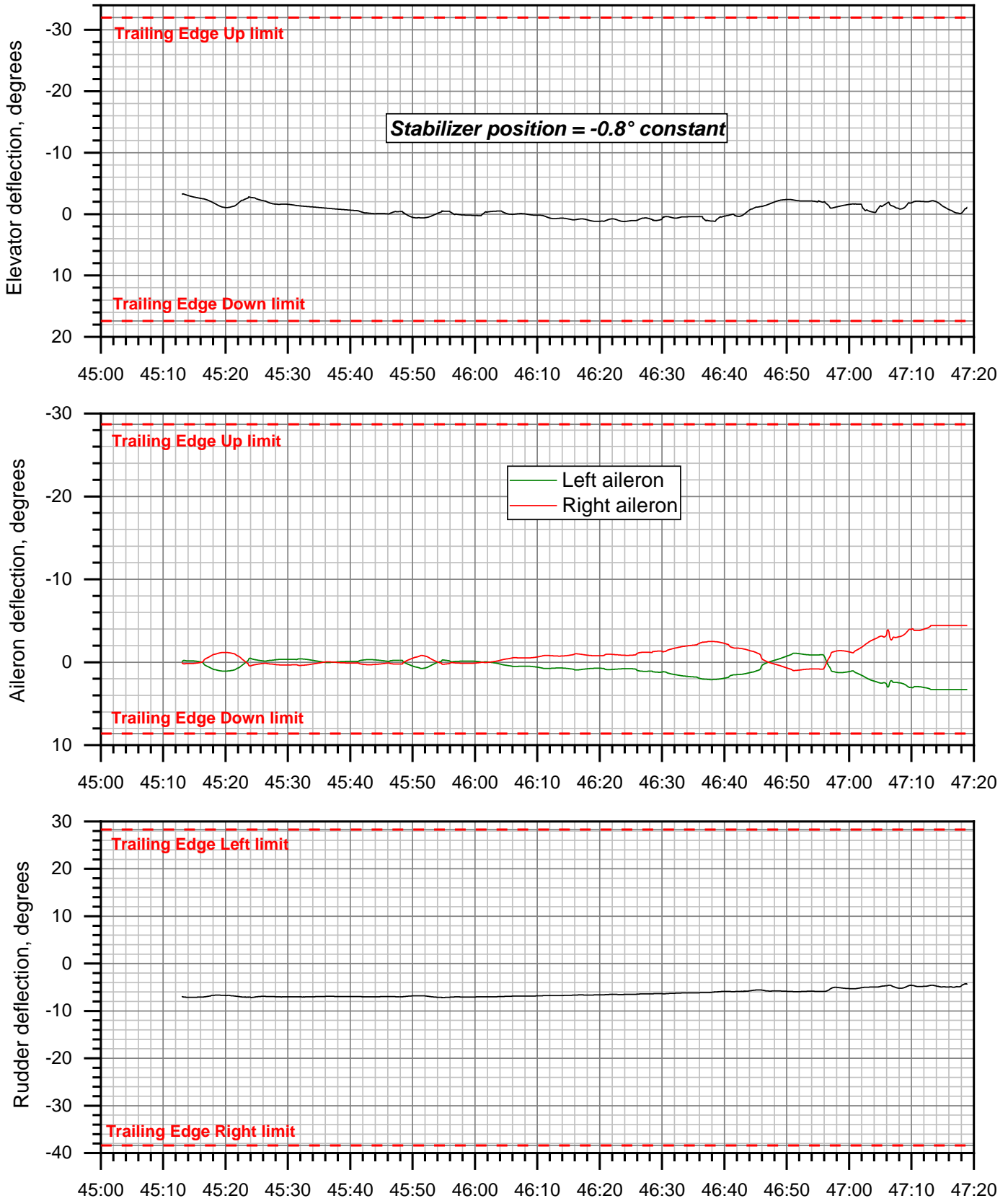


AMA ASR-11 time, MM:SS after 23:00:00 CDT

Figure 16.

# CEN17FA168: Pilatus PC-12, N933DC, Amarillo, TX, 04/28/2017

## Simulation control surfaces

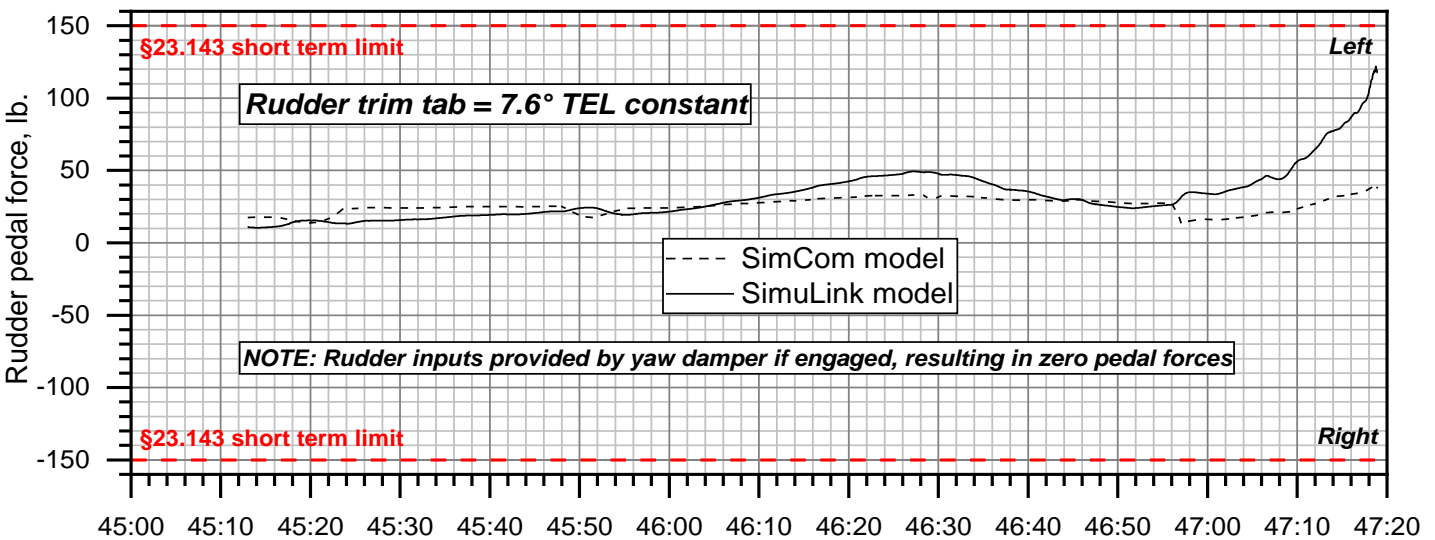
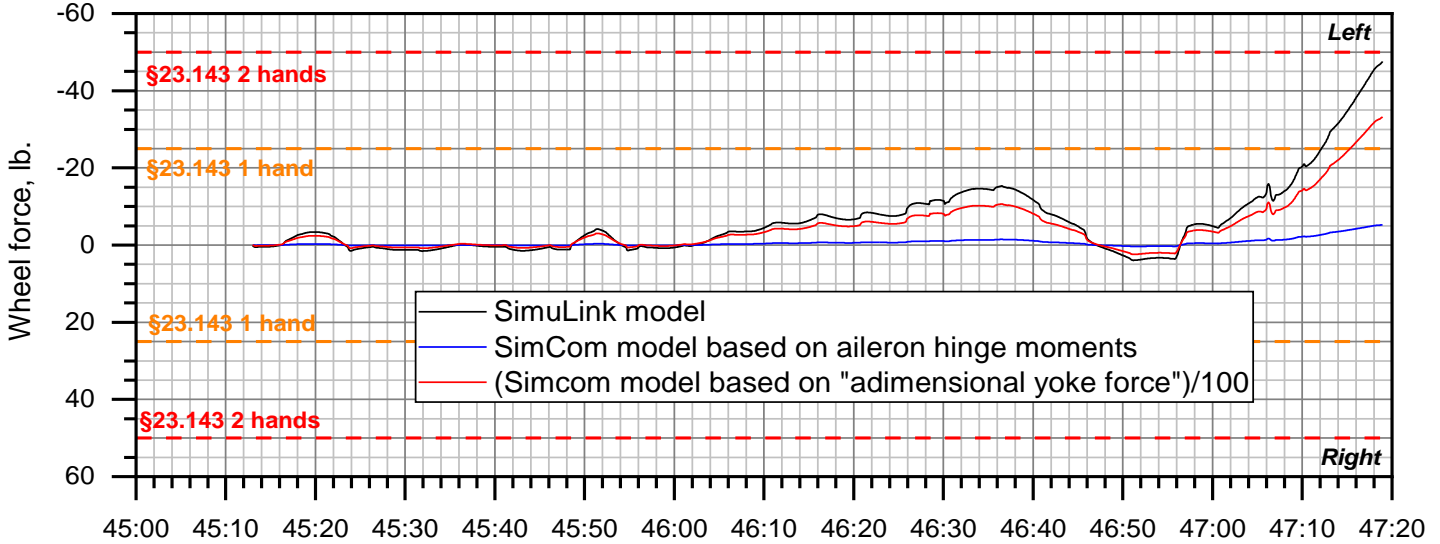
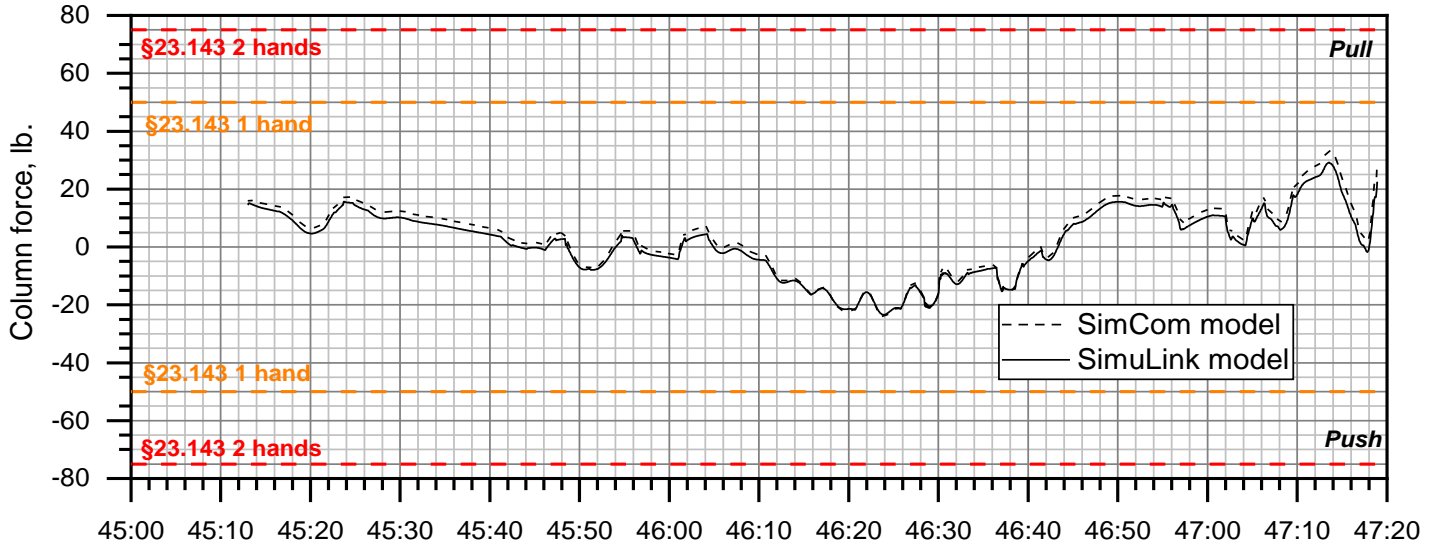


AMA ASR-11 time, MM:SS after 23:00:00 CDT

**Figure 17.**

# CEN17FA168: Pilatus PC-12, N933DC, Amarillo, TX, 04/28/2017

## Simulation control forces



AMA ASR-11 time, MM:SS after 23:00:00 CDT

Figure 18.



**Figure 19.** Cockpit trim indicator showing horizontal stabilizer position consistent with condition of stabilizer actuator found in wreckage, per Reference 5. Green trapezoid (“sector”) = neutral position; green diamond = takeoff position. Simulation stabilizer set constant at neutral position.

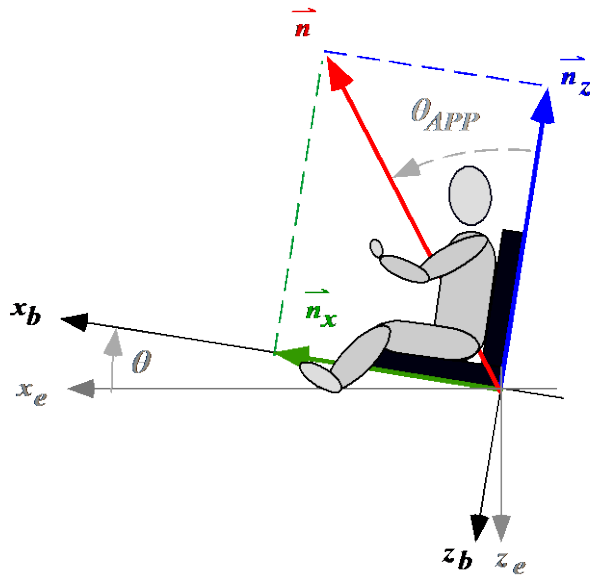


**Figure 20a.** Load factor vector  $\vec{n}$  in an accelerated reference frame. Note that for  $n_x > 0$ ,  $\theta_{APP} > \theta$ .

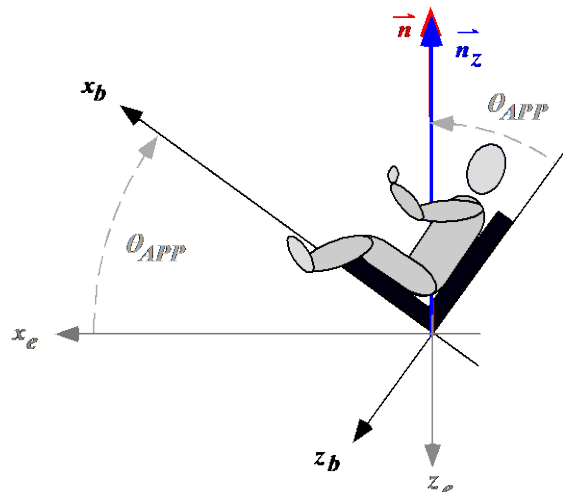


**Figure 20b.** Equivalent load factor vector  $\vec{n}$  in an unaccelerated reference frame.